

# Perturbative Color Correlations in Double Parton Scattering.

B. Blok\* and J. Mehl†

*Department of Physics, Technion – Israel Institute of Technology, Haifa, Israel*

We study the contribution of color correlations to Double Parton Scattering (DPS). We show that there is a specific class of Feynman diagrams related to so called  $1 \rightarrow 2$  processes when the contribution of these color correlations is not Sudakov suppressed with the transverse scales. The effective absence of Sudakov suppression gives hope that although they are small relative to color singlet correlations, they eventually can be observed.

arXiv:2210.13282v2 [hep-ph] 11 May 2024

---

\* blok@physics.technion.ac.il

† yonatanm@campus.technion.ac.il

## CONTENTS

I. Introduction	3
II. pQCD Formalism	7
A. Color Non-Singlet DGLAP equation	7
B. Generalized Parton Distribution	12
C. $1 \rightarrow 2$ for Color Non-Singlet Channels	14
Self Consistency of the $\alpha_{[1]} \overline{D}_h^{AB}$ Normalization	18
D. Regularization of $z_i \rightarrow 1$ Singularity	20
III. Numerics	22
IV. Conclusion	25
Acknowledgments	26
A. Color Kernels	26
1. Color Factor for the $8_a$ Representation	27
a. $\overline{C}_G^G$	28
b. $\overline{C}_F^G$	29
c. $\overline{C}_F^F$	30
d. $\overline{C}_G^F$	30
2. Color Factor for the $8_s$ Representation	31
a. $\overline{C}_G^G$	31
b. $\overline{C}_F^G$	32
c. $\overline{C}_F^F$	33
d. $\overline{C}_G^F$	33
3. Normalization of $\overline{C}_F^G$ and $\overline{C}_G^F$	34
a. $8_a$	35
b. $8_s$	35
B. Formal Derivation of the Non-Singlet DGLAP Equation	36
C. $\tilde{D}_A^B$ at the Limit $x \rightarrow 1$	38
D. Regularizing Divergent Integrals	44

E. Rules for Color Projectors	46
1. Exact Form of Projectors	46
2. Properties	47
a. Projectors	47
b. Symmetries	47
c. Change in Basis	48
d. Interaction Force	50
e. Dimensions of the Representation	50
f. Completeness Relation	51
3. Proof of Incoming-Outgoing Symmetry	51
F. Comments on Different Formalisms	51
1. The Sudakov Suppression Factor.	51
a. Proof of the Singlet Case	52
b. The non-Singlet Case.	53
c. Different Sudakov Factors	55
2. Regularization of $z \rightarrow 1$ divergence	56
References	59

## I. INTRODUCTION

The theory of double parton scattering (DPS) in QCD was the subject of intensive development in recent years. The first work on DPS was done in the early 80s [1, 2], and the first detailed experimental observations of DPS were done in Tevatron. Recently new detailed experimental studies of DPS were carried out at LHC while a new theoretical formalism based on pQCD was developed [3–11]. In these works, the fundamental role of parton correlations in DPS scattering was realized and estimated and new physical objects to study these correlations - two particle generalized parton distribution ( ${}_2GPD$ ) were introduced. However, most of this work was devoted to the study of color singlet correlations in DPS processes.

Recently, a lot of interest was attended to color non-singlet correlations in proton-proton collisions. The possibility of such correlations was already discussed in the 80s [12, 13]. However, it was shown that such correlations are strongly Sudakov suppressed due to a need to change color quantum numbers between the amplitude and the complex conjugate [12, 13]. The color correlations

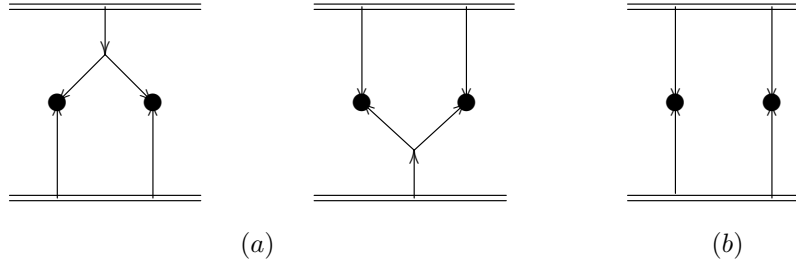


Figure 1. The different diagrams contributing to double parton scattering (DPS) (a) the two possible 1 + 2 processes and (b) a 2 + 2 process. As explained in the text there is no “1 + 1” contribution. the = line represents the hadrons

were shown to be suppressed as

$$\exp\left(-\alpha_s \log^2\left(\frac{Q^2}{\Lambda_{QCD}^2}\right)\right) \quad (1)$$

where  $Q$  is the transverse momenta. As a result, such correlations are negligible, at least in conventional hard processes, and rapidly decrease with hard scale. Such correlations were first considered in [12, 13] for conventional hard processes, and for the so-called  $2 \rightarrow 2$  processes in the DPS (see figure 1 (b)).

More recently it was realized that the color correlations can occur also in the so-called  $1 \rightarrow 2$  processes and they were studied in [8, 11, 14–16]. In recent work [17] it was noted that the two particle  ${}_2GPD$  that described color non-singlet correlations can be negative.

Still, there remains a problem to find the contribution of color correlations in DPS processes. Indeed, the contribution of color correlations is Sudakov suppressed, so the appearance of color ladders in the scattering amplitudes is negligible for transverse momenta where one can expect to observe the DPS processes. On the other hand, the analysis of singlet correlations in DPS processes shows that a significant part of the contribution to  ${}_2GPD$  comes from the processes where the ladder splits into two short ladders, corresponding to the fundamental solutions of DGLAP equations for  $x \sim 1$ , leading to two hard processes. In these ladders, the transverse momenta evolve not from  $Q_0^2 \sim 0.5 \text{ GeV}^2$  to  $Q^2$ , but from  $k$  to  $Q^2$  Where  $Q_0 \ll k \ll Q$  of some indeterminate perturbative scale where the split occurred.

For such processes, one can consider the  $1 \rightarrow 2$  processes depicted in figure 2 (a). Indeed the two ladders coming from below in figure 1 (a), and the ladder that splits are not suppressed. Only two ladders that go to hard processes after the split are colored and will be suppressed, but Sudakov

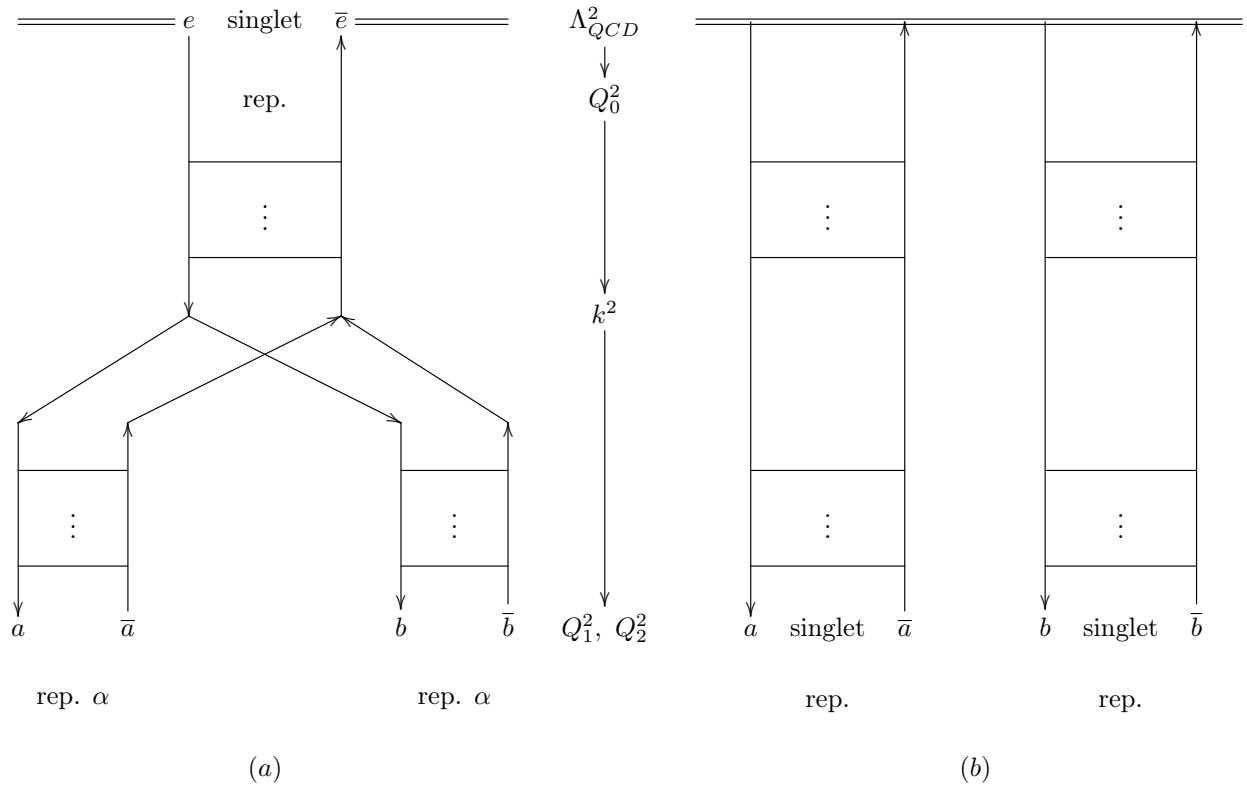


Figure 2. (a) The  $1 \rightarrow 2$  process diagram and its complex conjugate with the DGLAP ladders presented explicitly. Both parton pairs  $a, \bar{a}$  and  $b, \bar{b}$  are in some nonsinglet representation  $\alpha$  while  $e, \bar{e}$  are in a singlet state. (b) the  $2 \rightarrow 2$  diagram and its complex conjugate, now  $a, \bar{a}$  and  $b, \bar{b}$  are in a singlet representation because other representations are Sudakov suppressed. The scales of the ladder evolution are shown in middle.

suppression may be much smaller

$$\sim \exp\left(-\alpha_s \log^2\left(\frac{Q^2}{k^2}\right)\right). \quad (2)$$

In this paper we shall calculate  ${}_2GPD$  corresponding to such processes, and find that such  ${}_2GPD$  may be indeed large - up to 5-10% relative to singlet  ${}_2GPD$ , extensively studied before [9, 18]. Moreover, this contribution does not decrease with  $Q^2$  and slowly increases relative to mean field contribution to  ${}_2GPD$  like for color singlet  $1 \rightarrow 2$  processes, thus being present at Tevatron and LHC. We shall see that these contributions can be both positive and negative, depending on the representation of color  $SU(3)$ .

We shall see that the characteristic scale where the singlet ladder in  $1 \rightarrow 2$  is increasing with the hard scale  $Q$  of the process. This is contrary to singlet split scale, which does not depend on

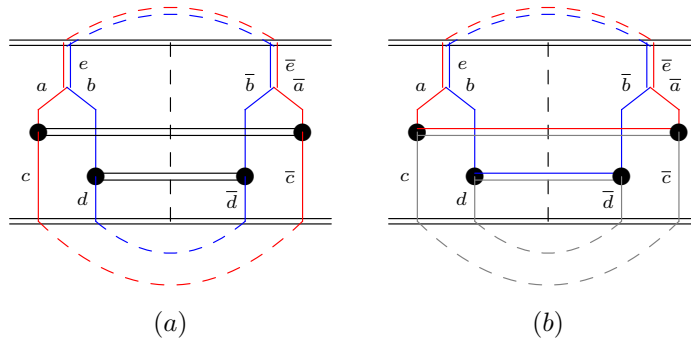


Figure 3. Different amplitudes (diagram contracted with it's complex conjugate) that contribute to the  $1+2$  process. Color flow is schematically shown using the red and blue lines for color neutral final states ( $a$ ) and final states that carry color numbers ( $b$ ). The  $=$  lines represent the final states. Particles in a singlet state are contracted explicitly by a dashed line (we assume, as will be discussed in the text, that particles not coming from  $1 \rightarrow 2$  processes, i.e the bottom part of the graphs, are in singlet state due to strong Sudakov suppression of the non-singlet states). It can be seen that only the singlet structure (i.e  $a$  is with the same color as  $\bar{a}$  and so are  $b$  and  $\bar{b}$ ) can contribute, unless one assume a "1+1" type amplitude or a non-singlet non-perturbative distribution.

the energy and is of order several GeV. Due to such energy dependence of the split scale in colour channels, the corresponding  $1 \rightarrow 2$  part of  ${}_2GPD$  is effectively not suppressed.

As a result, we shall have the so called  $1v1$  [19] processes with two singlet ladders from above and below (i.e. from each of contributing nucleons) split into two colour ladders, being unsuppressed with the energy scale increase. Indeed, such contributions were recently considered in [20]. Nevertheless further work is needed in order to observe the contributions of these processes and distinguish them from both conventional singlet DPS and conventional  $1 \rightarrow 1$  hard processes.

In our calculations, we use "DDT-like" formalism [21].

In our numerical calculations of  ${}_2GPD$ , we concentrate on gluonic  ${}_2GPD$  since they give a dominant contribution to the considered processes due to the large color factor, and neglect the contribution of quark and mixed quark-gluon  ${}_2GPD$ .

The paper is organized in the following way. In Section II we describe our formalism to calculate the color correlated  ${}_2GPD$  in LLA. We study the nonsinglet analogue of DGLAP equation and the  $x \rightarrow 1$  asymptotic of its fundamental solutions. We show how to calculate nonsinglet  ${}_2GPD$  for  $1 \rightarrow 2$  processes using the fundamental singlet and nonsinglet solutions of the DGLAP equation. We explain the divergences in the integrals for  ${}_2GPD$  and show that these integrals can be calculated using an analytical continuation procedure.

In Section III we use the results of Sections II, to calculate the non singlet distribution. Our results are summarized in the conclusion.

In Appendix A we review the calculation of DGLAP kernels for nonsinglet channels. Although the results for kernels are known we believe it is useful to give the details of derivations. In Appendix B we rederive nonsinglet DGLAP equation and show that the contributions of real and virtual emissions have different color factors, thus leading to Sudakov suppression [12, 13]. In Appendix C we study the relevant asymptotic for  $x \rightarrow 1$  for colored channels. In Appendix D we discuss the divergent integrals in  ${}_2GPD$  and explained their regularization using theory of generalized functions. In Appendix E we review the properties of color projectors relevant to the calculations done in this paper. In Appendix F we comment on the relation between other formalisms used in the literature and the one used in this paper.

## II. PQCD FORMALISM

In this section, we'll develop the formalism for computing the  $1 \rightarrow 2$  distribution when the two partons are color correlated. First, we review the derivation of the DGLAP equation [25–27] for non-singlet color states and discuss the solutions to this equation, in particular the fundamental solutions (i.e. with initial conditions of the form  $\sim \delta(x - 1)$  in the  $x \rightarrow 1$  limit). Then we express the two particle  ${}_2GPD$  for arbitrary color states, connected with the  $1 \rightarrow 2$  processes, through the solutions of the non-singlet DGLAP. This analysis will include divergent integrals, which we explain how to regularize.

### A. Color Non-Singlet DGLAP equation

Consider first the conventional singlet DGLAP equation [25–27]. The evolution of a parton A from one energy scale  $k_0^2$  to another parton B at scale  $Q^2$  (the hard scale of the process) with a fraction of longitudinal momentum  $x$  (the Bjorken variable, which is the fraction of longitudinal momentum of the parton compared to the parent hadron) is described by the structure function  $D_A^B(x, k_0^2, Q^2)$  (in the following we'll suppress unnecessary inputs). We take the hard scale  $Q^2$  to be the transverse scale  $p_\perp^2$  (which is the transverse momentum of one of the outgoing particles squared). The exact choice of  $Q^2$  gives only next to leading order effects and therefore is not within the scope of this work. In a physical gauge  $D_A^B$  receives contributions from both real (ladder) and virtual (self energy) diagrams which result in the DGLAP equation:

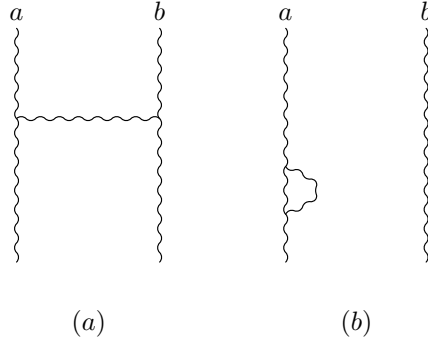


Figure 4. Example of different contributions to the DGLAP equation. (a) the real (ladder) diagram for  $\Phi_G^C$ , the color factor for this diagram might depend on the color state of the gluons  $a, b$ . (b) example of a virtual (self-energy) contribution, these contributions do not depend on the color state of  $a, b$ .

$V_F^F$	$2 \cdot \frac{1+z^2}{1-z}$
$V_F^G$	$2 \cdot \frac{1+(1-z)^2}{z}$
$V_G^F$	$2 \cdot [z^2 + (1-z)^2]$
$V_G^G$	$4 \cdot [z(1-z) + \frac{1-z}{z} + \frac{z}{1-z}]$

Table I. Longitudinal Momentum dependence of the DGLAP kernels in leading order

$$\frac{\partial D_A^B(x, Q^2)}{\partial \ln(Q^2)} = \frac{\alpha_s(Q^2)}{4\pi} \sum_C \int_0^1 \frac{dz}{z} \left[ \underbrace{\Phi_C^B(z) D_A^C\left(\frac{x}{z}, Q^2\right)}_{\text{real contributions}} - \underbrace{\Phi_B^C(z) z^2 D_A^B(x, Q^2)}_{\text{virtual contributions}} \right]. \quad (3)$$

The initial conditions for (3) are  $D_A^B(x, k_0^2, k_0^2) = \delta_A^B \delta(1-x)$  which represents the fact we are looking for the fundamental solutions (or Green functions) for these equations.  $A, B, C$  are the different types of partons (quarks, anti-quarks or gluons) and the sum  $\sum_C$  runs over gluons and all  $n_f$  flavors of quarks and anti-quarks ( $n_f$  is the number of active flavors).  $\Phi_A^C$  are the DGLAP kernels without the “+ subscription” [21] and are given by  $\Phi_A^C(z) = C_A^C \cdot V_A^C(z)$ . Here  $V_A^C$  is given in table I and  $C_A^C = {}^1\bar{C}_A^C$  are the color factors given in table II for the singlet ( $\alpha = 1$ ) column.  $\alpha_s(k^2)$  is the strong coupling constant and is given to leading order by:

$$\alpha_s(k^2) = \frac{12\pi}{\beta_0 \cdot \ln\left(\frac{k^2}{\Lambda_{QCD}^2}\right)}, \quad (4)$$

with  $\Lambda_{QCD} = 0.22 \text{ GeV}$  and  $\beta_0 = 11 \cdot N - 2 \cdot n_f$ .  $N$  is the number of colors, we take both  $N$  and



$\alpha =$	1	$8_a$	$8_s$	10	27	0
$\alpha \overline{C}_F^F$	$\frac{N^2-1}{2N}$	$-\frac{1}{2N}$	$-\frac{1}{2N}$	0	0	0
$\alpha \overline{C}_F^G$	$\frac{N^2-1}{2N}$	$\sqrt{\frac{N^2-1}{8}}$	$\frac{1}{2N} \sqrt{\frac{(N^2-4)(N^2-1)}{2}}$	0	0	0
$\alpha \overline{C}_G^F$	$\frac{1}{2}$	$\frac{1}{2} \sqrt{\frac{N^2}{2(N^2-1)}}$	$\frac{1}{2} \sqrt{\frac{N^2-4}{2(N^2-1)}}$	0	0	0
$\alpha \overline{C}_G^G$	$N$	$\frac{N}{2}$	$\frac{N}{2}$	0	-1	1

Table II. Color factors for different representations. In this paper, we consider only irreducible representations, except for the two gluon decuplet representations where we combine them together and denote  $10 := 10 + \overline{10}$ .

$n_f$  to be 3 in the numeric calculations. All the diagrams in this paper will be computed to leading order in  $\alpha_s$  and the evolution equations are within the LLA (Leading Logarithmic Approximation).

We now consider the case where the evolving parton and its complex conjugate are not in a singlet state. To be more specific assume they form together some non-singlet irreducible color representation  $\alpha$  (here and for the rest of the paper we denote color representations with Greek letters). Then the virtual and real contributions receive different color factors as is shown in figure 4 (as it was first stressed in [12, 13]). We therefore, get the non-singlet DGLAP equation for irreducible  $SU(3)$  representation  $\alpha$  (note the representation index is to the left of the quantities in this equation, i.e  $\alpha X$ ):

$$\frac{\partial \alpha \overline{D}_A^B(x, Q^2)}{\partial \ln(Q^2)} = \frac{\alpha_s(Q^2)}{4\pi} \sum_C \int_0^1 \frac{dz}{z} \left[ \underbrace{\alpha \overline{\Phi}_C^B(z)}_{\text{new kernel}} \alpha \overline{D}_A^C\left(\frac{x}{z}, Q^2\right) - z^2 \underbrace{\Phi_B^C(z)}_{\text{old kernel}} \alpha \overline{D}_A^B(x, Q^2) \right]. \quad (5)$$

Here  $\Phi_A^C$  are the conventional singlet DGLAP kernels (as described above). On the other hand  $\alpha \overline{\Phi}_A^C$  are the new kernels for the representation  $\alpha$ , coming from the real radiation (consequently they appear in the first term, on the right hand side). These kernels have the same momentum ( $z$ ) dependence as the singlet ones but have a different color factor:

$$\alpha \overline{\Phi}_A^C(z) = \alpha \overline{C}_A^C \cdot V_A^C(z). \quad (6)$$

These factors were computed in [8] (we also write an expanded explanation in Appendix A) and are shown in table II.

Note that while writing the kernels in table I we use the same regularisation as in [21] for terms singular when  $z \rightarrow 1$ :

$$1 - z \rightarrow 1 - z + \Delta, \Delta = k_0^2/\sigma_k \sim k_0^2/Q^2 \quad (7)$$

As it was shown in [21] (5) includes both double logarithmic and single logarithmic terms in hard transverse scale. For the singlet case double logarithmic terms do not contribute. Eq. (5) is well defined after regularisation (7). We can now formally solve this equation using the ansatz:

$${}^\alpha \bar{D}_A^B(x, k_0^2, Q^2) = {}^\alpha \bar{S}_A(k_0^2, Q^2) {}^\alpha \tilde{D}_A^B(x, k_0^2, Q^2). \quad (8)$$

If we take for  ${}^\alpha \bar{S}_A(k_0^2, Q^2)$  the expression

$${}^\alpha \bar{S}_A(k_0^2, Q^2) = e^{-\sum_C (C_A^C - \alpha \bar{C}_A^C) \int_{k_0^2}^{Q^2} \frac{dk^2}{k^2} \frac{\alpha_s(k^2)}{4\pi} \int_0^1 dz z V_A^C(z)} \quad (9)$$

we obtain that the function  $\tilde{D}$ , which we call the "tree level factor", satisfies the Equation

$$\frac{\partial {}^\alpha \tilde{D}_A^B(x, Q^2)}{\partial \ln(Q^2)} = \frac{\alpha_s(Q^2)}{4\pi} \sum_C \int_0^1 \frac{dz}{z} \left[ \underbrace{{}^\alpha \bar{\Phi}_C^B(z)}_{\text{new kernel}} {}^\alpha \tilde{D}_A^C\left(\frac{x}{z}, Q^2\right) - z^2 \underbrace{{}^\alpha \bar{\Phi}_B^C(z)}_{\text{new kernel}} {}^\alpha \tilde{D}_A^B(x, Q^2) \right]. \quad (10)$$

which has the form of the conventional DGLAP equation and can be solved by the standard method [21].

Consider first the function  ${}^\alpha \bar{S}_A$ . The direct calculation shows that for DDT regularisation its logarithm is a sum of two pieces: the universal piece leading to a form factor

$${}^\alpha \bar{S}_A(k_0^2, Q^2) \approx e^{-\left(C_A^A - \alpha \bar{C}_A^A\right) \cdot \frac{12}{\beta_0} \left[ \log \frac{Q^2}{\Lambda_{QCD}^2} \log \left[ \frac{\log \frac{Q^2}{\Lambda_{QCD}^2}}{\log \frac{k_0^2}{\Lambda_{QCD}^2}} \right] - \log \frac{Q^2}{k_0^2} \right]}, \quad (11)$$

that coincides with a Sudakov form factor obtained in [28]. This piece comes from neglecting the nonsingular terms in integration of the kernels  $V(z)$  in  $z$  from 0 to 1, i.e. leaving only  $1/(1-z+\Delta)$ . There is additional nonuniversal piece that is single logarithmic and is obtained by integration of nonsingular part of the kernel  $V$  over  $z$ . It is interesting to note that numerically the form factor (11) is very close to simple double logarithmic expression used in [13]

$${}^\alpha \bar{S}_A(k_0^2, Q^2) = e^{-\frac{\alpha_s}{2\pi} (C_A^A - \alpha \bar{C}_A^A) \ln^2 \left( \frac{Q^2}{k_0^2} \right)}. \quad (12)$$

The corrections due to nonsingular parts of the kernel were calculated explicitly for all channels that we considered and numerically they contributed less than 10 percent to S. For more detailed discussion of single logarithms and comparison to the formalism [8, 11, 15] see Appendix F.

We can now move to the solution of the DGLAP equation for  $\tilde{D}$ . Equation (10) has the same form as the conventional singlet DGLAP equation (3) but with different color factors. To solve this equation we simply repeat the steps for solving the regular DGLAP equations [21] and by the analytical continuation of the arguments replace the singlet color factors  $C_A^B$  with the new, representation dependent,  ${}^\alpha\bar{C}_A^B$ . To be more concrete:

- Transform to Mellin space using

$${}^\alpha\tilde{D}_A^B(j) = \int {}^\alpha\tilde{D}_A^B(x, k_0^2) x^{j-1} dx \quad (13)$$

and change variables from  $k_0$  and  $Q$  to  $\xi = \frac{3}{\beta_0} \ln \left[ \frac{\alpha_s(k_0^2)}{\alpha_s(Q^2)} \right]$  ( $\beta_0$  is defined above).

- Equation (10) then transform to a linear system of first order differential equations in  $\xi$  ( $(1 + 2n_f)^2$  equations, for each combination of  $A, B$ , each can be a gluon or any of  $n_f$  fermions or anti-fermions). The system has a Hamiltonian  $H$  (a  $(1 + 2n_f) \times (1 + 2n_f)$  matrix) that only depends on  $j$  and can be worked out analytically. The solution to this system is simply  $\exp(\xi H)$ .
- Solve  ${}^\alpha\tilde{D}_A^B(j, \xi)$  analytically by diagonalizing  $H$ , taking the exponent at this base, and then transforming it back. We get that  ${}^\alpha\tilde{D}_A^B(j, \xi)$  will be a linear combination of exponents of the eigenvalues of  $\xi H$  (there are only 3 independent eigenvalues).
- Return to  $x$  space using the (numeric) inverse Mellin transform:

$${}^\alpha\tilde{D}_C^B(x, \xi) = \int_{-\infty}^{\infty} \frac{dj}{2\pi i} x^{-j\alpha} \tilde{D}_C^B(j, \xi). \quad (14)$$

This integral must be taken to the right of every singularity of  ${}^\alpha\tilde{D}_C^B(j, \xi)$ . For numerical purposes we take [25, 29]

$$j(t) = \text{Max} \left[ 1.5, \frac{16}{3} \frac{C_F^F}{1-x} \right] + \begin{cases} (i-1)t & t > 0 \\ (1+i)t & t < 0 \end{cases}. \quad (15)$$

Note that although  ${}^\alpha\tilde{D}_A^B$  can be written only as a function of  $x$  and  $\xi$ , which encode the dependence on both  $k_0$  and  $Q$ , this is not true for  ${}^\alpha\bar{D}_A^B(x, k_0^2, Q^2)$  due to the Sudakov factor.

To conclude: the solution  ${}^\alpha\bar{D}_A^B$  to the non-singlet DGLAP equation (5) is a Sudakov suppression factor  ${}^\alpha\bar{S}_A$  given in (9) times  ${}^\alpha\tilde{D}_C^B$ , the solution of (10), which can be numerically evaluated for each value of  $x$ ,  $k_0^2$  and  $Q^2$  in a given representation. It's important to note that for non-singlet state  ${}^\alpha\bar{D}_A^B$  no longer represents a physical distribution and therefore might even be negative [17].

For the region  $x \sim 1$ , if  ${}^\alpha\bar{C}_A^A > 0$  we can analytically solve (10) using the saddle point method [21] (see also Appendix C for detailed derivation). The saddle point for the inverse Mellin transform integral is  $j_0 = \frac{4\xi^\alpha\bar{C}_A^A}{1-x} \gg 1$  which is on the right of all the singularities of  $\tilde{D}(j)$ . We then get an analytical expression for  $\tilde{D}_F^F(x, \xi)$  and  $\tilde{D}_G^G(x, \xi)$  at this region. For the case  ${}^\alpha\bar{C}_A^A \leq 0$  this argument does not hold, the saddle point  $j_0$  is then negative and therefore cannot be taken as the primary value for the inverse integral (which must be taken to the right of every singularity). However, we can take the analytical continuation of the analytical expression we got at the region  ${}^\alpha\bar{C}_A^A > 0$  (it's also satisfying to know that for the region  $x \sim 0.9 - 0.999$ , where  $\tilde{D}$  can be numerically evaluated to good accuracy, this analytical continuation proves to be a very good approximation):

$${}^\alpha\tilde{D}_F^F(x, \xi) \underset{x \sim 1}{=} \frac{e^{-\xi[(4\gamma_E - \frac{17}{3})^\alpha\bar{C}_F^F + \frac{8}{3}\alpha\bar{C}_F^G]}}{\Gamma(4\xi^\alpha\bar{C}_F^F)} \cdot \frac{1}{(1-x)^{1-4\xi^\alpha\bar{C}_F^F}} \quad (16a)$$

$${}^\alpha\tilde{D}_G^G(x, \xi) \underset{x \sim 1}{=} \frac{e^{\xi[(\frac{11}{3} - 4\gamma_E)^\alpha\bar{C}_G^G - \frac{4}{3}n_f\alpha\bar{C}_G^F]}}{\Gamma(4\xi^\alpha\bar{C}_G^G)} \cdot \frac{1}{(1-x)^{1-4\xi^\alpha\bar{C}_G^G}} \quad (16b)$$

Note that the dependence on  $x$  in the limit  $x \rightarrow 1$  is given by  $1-x$  to some power. We therefore see that taking the integral of these functions over  $x$  will diverge if  ${}^\alpha\bar{C}_A^A \leq 0$ . This will prove to be a problem in the next section, for which we introduce a regularization at section IID. The mixed gluon fermion fundamental solutions like  ${}^\alpha\tilde{D}_F^G$  are suppressed relative to diagonal ones by factors  $(1-x)$ . They are nonsingular and their contribution to two particle  ${}_2GPD$  for  $1 \rightarrow 2$  processes is negligible, so we shall not need the explicit expressions for them.

## B. Generalized Parton Distribution

Recall that the cross section of DPS is expressed through two particle Generalized Parton distributions. Consider first the singlet case [4, 7]. The generalized two parton distribution ( ${}_2GPD$ ) in a hadron is a sum of these two distributions [4, 7]

$$D(x_1, x_2, Q_1, Q_2, \vec{\Delta}) = [{}_1]\bar{D}_h(x_1, x_2, Q_1^2, Q_2^2) + [{}_2]\bar{D}_h(x_1, x_2, Q_1^2, Q_2^2, \vec{\Delta}). \quad (17)$$

Here  $x_1, x_2$  the Bjorken variables for the partons,  $Q_1, Q_2$  the transverse scales, and  $\vec{\Delta}$  is conjugated to the distance between the hard processes. The first term describes the  $2 \rightarrow 2$  processes when the two partons come directly from the nonperturbative wave function of the nucleon and then evolve from the hard process, while the second term corresponds to the parton from the nonperturbative wave functions that evolved to some perturbative scale  $k$  where it splits into 2 perturbative partons that evolve.

The total DPS cross section is schematically

$$\begin{aligned} \sigma_{DPS} = & \sigma_1 \sigma_2 \times \frac{\int d^2 \Delta}{(2\pi)^2} [2]D(x_1, x_2, Q_1, Q_2, \Delta) [2]D(x_3, x_4, Q_1, Q_2, \Delta) \\ & + [2]D(x_1, x_2, Q_1, Q_2, \Delta) [1]D(x_3, x_4, Q_1, Q_2, \Delta) + [1]D(x_1, x_2, Q_1, Q_2, \Delta) [2]D(x_3, x_4, Q_1, Q_2, \Delta). \end{aligned} \quad (18)$$

Note the absence of terms  $[1]D[1]D$  that do not contribute to LLA approximation [6, 7] (note however the discussion in [10] on the subject).

The first term in Eq. 17 can be calculated in the mean field approximation [4]:

$$[2]D_h^{AB}(x_1, x_2, Q_1^2, Q_2^2, \vec{\Delta}) = G_h^A(x_1, Q_1^2) G_h^B(x_2, Q_2^2) [F_{2g}(\vec{\Delta})]^2. \quad (19)$$

Here  $G(x, Q^2)$  are the parton distribution functions in the nucleon (PDFs) and  $F_{2g}(\vec{\Delta})$  is the so called ‘‘two gluon form factor’’ [30]. With good accuracy it will be enough to use the dipole parametrization of the two gluon form factor. In this parametrization the two gluon form factor has the form:

$$F_{2g}(\vec{\Delta}) = \left(1 + \frac{\Delta^2}{m_g^2}\right)^{-2}, \quad (20)$$

where  $m_g$  is a parameter that can be extracted from hadron photoproduction at the HERA and FNAL experiments, and is approximately  $m_g \approx 1.1 \text{ GeV}$  [4, 7, 30]. We neglect the weak dependence of  $m_g$  on  $Q^2$  and  $x$  (the dependence on  $x$  of individual  $m_g$  of different partons cancel out, and the remaining dependence on  $Q^2$  is negligible [30])

The DPS cross section for  $2 \rightarrow 2$  processes in the mean field approximation is usually written in the form

$$\sigma_{DPS} = \frac{\sigma_1 \sigma_2}{\sigma_{eff}}, \quad (21a)$$

$$\sigma_1 = G^G(x_1, Q_1^2) G^G(x_3, Q_1^2) \hat{\sigma}_1, \quad (21b)$$

$$\sigma_2 = G^G(x_2, Q_2^2) G^G(x_4, Q_4^2) \hat{\sigma}_2, \quad (21c)$$

where in the mean field approximation

$$\frac{1}{\sigma_{eff}} = \int \frac{d^2\vec{\Delta}}{(2\pi)^2} \left[ F_{gg}(\vec{\Delta}) \right]^4 = \frac{m_g^2}{28\pi}. \quad (22)$$

Consider now the calculation of  $1 \rightarrow 2$  part of the cross section, corresponding to the second and third terms in Eq. 18. The integral over  $\vec{\Delta}$  can be easily taken since the two gluon form factors decrease much more rapidly with  $\vec{\Delta}$  than perturbative  ${}_2GPD$ , that can be taken at the point  $\vec{\Delta} = 0$ . The  $\vec{\Delta}$  integral is easily taken giving the fact that

$$\int \frac{d^2\vec{\Delta}}{(2\pi)^2} \left[ F_{gg}(\vec{\Delta}) \right]^2 = \frac{m_g^2}{12\pi}. \quad (23)$$

So the  $1 \rightarrow 2$  part of the cross section is

$$\sigma_{DPS}^{1 \rightarrow 2} = \hat{\sigma}_1 \hat{\sigma}_2 \frac{m_g^2}{12\pi} (G(x_3, Q_1^2) G(x_4, Q_2^2)_{[1]} D(x_1, x_2, Q_1^2, Q_2^2, 0) + G(x_1, Q_1^2) G(x_2, Q_2^2)_{[1]} D(x_3, x_4, Q_1^2, Q_2^2, 0)) \quad (24)$$

Note that we get “geometric” enhancement of  $1 \rightarrow 2$  relative  $2 \rightarrow 2$  by a factor  $2 \times \frac{7}{3}$ , where factor 2 comes from two terms in (24).

These results can be immediately extended to color correlations. We define the free indexed  ${}_{[2]}D_{h;AB}^{a\bar{a}b\bar{b}}$ ,  ${}_{[1]}D_{h;AB}^{a\bar{a}b\bar{b}}$  (see figure 5). These  ${}_2GPD$ 's are normalized as:

$${}_{[2]}D_{h;AB}^{a\bar{a}b\bar{b}} = {}_{[2]}D_h^{AB} P_{a\bar{a};b\bar{b}}^1 \quad (25)$$

for singlet case, where  $P^1$  is a color projector into the singlet representation.

Note that due to Sudakov suppression [12, 13] the colored  ${}_{[2]}D$  are small and we shall take into account only the singlet  ${}_2GPD$  in the  $2 \rightarrow 2$  part of the DPS process. For the  ${}_{[1]}D$  case non-singlet distributions might have weaker suppression (as explained in the introduction). We shall show and compute them explicitly in the next section.

### C. $1 \rightarrow 2$ for Color Non-Singlet Channels

Using the DDT [25] approximation for TMD (transverse momentum distribution) one can get a formulation for the contribution to the cross section from  $1 \rightarrow 2$  process, i.e  ${}_{[1]}D_h$ , when all ladders contributing to the evolution equations are the singlet ones [7, 9].

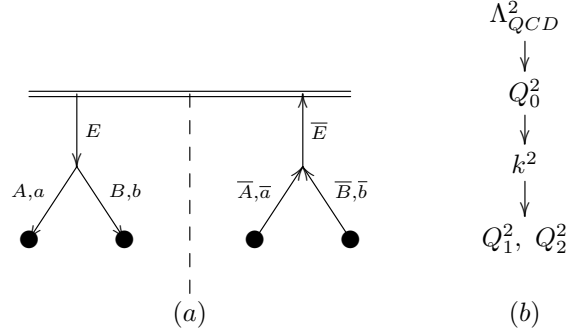


Figure 5. (a) General diagram for the  $1 \rightarrow 2$  process and its complex conjugate, the line represents either a quark or a gluon and the  $\bullet$  represents the hard process. The indices  $E, \bar{E}, A, \bar{A}, B, \bar{B}$  represent the types of the partons while  $a, \bar{a}, b, \bar{b}$  represent the color indices of this parton (these indices could be either quark or gluon indices). (b) the different characteristic energy scales of each part of the process.

This analysis can be generalized to non-singlet evolution  ${}_{[1]}D_{h;AB}^{a\bar{a}b\bar{b}}$  as described above. Define the  $t$ -channel [13, 17] distribution function as shown in figure 6:

$${}_{[1]}^{\alpha}\bar{D}_h^{AB} = \frac{1}{K^{\alpha}} P_{a\bar{a};b\bar{b}}^{\alpha} {}_{[1]}D_{h;BC}^{a\bar{a}b\bar{b}}. \quad (26)$$

Here  $P^{\alpha}$  is the projector of the color representation  $\alpha$ , and we normalized the projectors by  $K^{\alpha} = P_{c\bar{c};c\bar{c}}^{\alpha}$  - the dimension of the representation  $\alpha$  (see Appendix E for explicit values of  $K^{\alpha}$ ). The completeness relation of the color projectors asserts that:

$${}_{[1]}D_{h;AB}^{a\bar{a}b\bar{b}} = \sum_{\alpha} {}_{[1]}^{\alpha}\bar{D}_h^{AB} P_{a\bar{a};b\bar{b}}^{\alpha}, \quad (27)$$

as was the case for  ${}_{[1]}D_{h;AB}^{a\bar{a}b\bar{b}}$  in (25). We shall take a closer look at the normalization of  ${}_{[1]}^{\alpha}\bar{D}_h^{BC}$  when computing them, the self consistency of this normalization will be checked in Section II C. This relation means we can look at the contribution of each representation alone and then sum them together to get the total contribution from the  $1 \rightarrow 2$  process.

The distribution for this process when  $\alpha = 1$  (i.e,  $a, \bar{a}$  and  $b, \bar{b}$  are in a singlet state) was obtained in [7, 9] as:

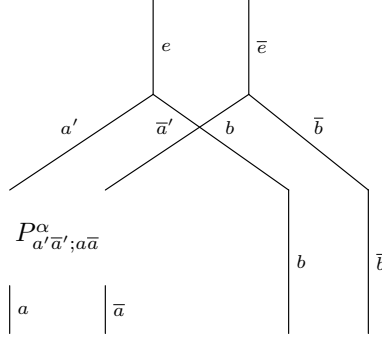


Figure 6. General diagram for the  $1 \rightarrow 2$  process and its complex conjugate, with a projector of the representation  $\alpha$  between them.

$$\begin{aligned}
 {}_{[1]}^1 \bar{D}_h^{AB}(x_1, x_2, Q_1, Q_2) &= \sum_{E, A', B'} \int_{Q_0^2}^{\min(Q_1^2, Q_2^2)} \frac{dk^2}{k^2} \frac{\alpha_s(k^2)}{2\pi} \int \frac{dy}{y} G_h^E(y; k^2) \\
 &\times \int \frac{dz}{z(1-z)} \Phi_E^{A'}(z) D_{A'}^A\left(\frac{x_1}{zy}; Q_1^2, k^2\right) D_{B'}^B\left(\frac{x_2}{(1-z)y}; Q_2^2, k^2\right).
 \end{aligned} \tag{28}$$

Here (See figure 5 for notations):

- The sum over  $E, A', B'$  runs over gluons and fermions but only if the splitting  $E \rightarrow A', B'$  is allowed by LO QCD.
- $k^2$  is the scale at which the splitting occurs,  $Q_0$  is some minimal scale which we take to be  $Q_0 = 0.7 \text{ GeV}$  and  $Q_1, Q_2$  the transverse scales and  $x_1, x_2$  the Bjorken variables.
- $G_h^E$  are the parton distribution functions (PDF's) of the hadron  $h$ , we take their values as given in [31, 32].
- $D$  are the solutions of the singlet DGLAP equation (3), and  $\Phi_E^{B'}$  are the singlet splitting functions.

Now assume we put the color projector of some other non-singlet representation  $\alpha \in \{8_a, 10, 1, 8_s, 27, 0\}$  as explained in (26). This projector means we need to change the evolution functions  $D_{A'}^A$  to the (representation dependent) non-singlet evolution  ${}^\alpha \bar{D}_{A'}^A$  that solves the non singlet DGLAP equation



(5). The color “flows” through this diagram so the evolution function for the partons  $B, \bar{B}$  must be in the same representation  $\alpha$  as the one for  $A, \bar{A}$  so we also change  $D_{B'}^B \rightarrow \alpha \bar{D}_{B'}^B$ . This argument follows from the processes we have chosen to minimize Sudakov suppression: the initial ladder that splits into two nonsinglet ones is itself a singlet. Unlike  $B$  and  $A$  the evolution of  $E$  is still governed by singlet ladders, as  $E$  and  $\bar{E}$  in figure 5 are directly connected and not through a projector, so  $G_h^E$  stays the same as in the singlet case.

The last change we need to account for is the splitting vertex  $\Phi_E^{A'}(z) = C_E^{A'} \cdot V_E^{A'}(z)$ . The momentum part  $V$  stays the same as it's not color dependent. The color factor however needs to be changed as it's no longer equivalent to a singlet splitting. Looking at the process from the point of view of particle  $A$  the splitting is exactly like a ladder  $\bar{\Phi}_{A'}^{B'}$  but with one difference. In a regular ladder, we average over the initial particle color state and sum over both the final and the ladder particle color state. But in this diagram, we should still sum over the color state of the particles  $A, B$  and average over that of  $E$ . To conclude the color factor must compensate for that, and we get a total color factor of:

$$\frac{n_{A'} \alpha \bar{C}_{A'}^{B'}}{n_E} \quad (29)$$

Here we define  $n_F = N$ ,  $n_G = N^2 - 1$  is the number of color states for the parton.  $\alpha \bar{C}_{A'}^{B'}$  are defined in table II. The choice to look from the point of particle  $A$  and not from  $B$  is of course arbitrary, but our choice of color factors makes sure the result is the same either way:

$$\frac{n_{A'} \alpha \bar{C}_{A'}^{B'}}{n_E} = \frac{n_{B'} \alpha \bar{C}_{B'}^{A'}}{n_E} \quad (30)$$

To conclude we write the non-singlet  $1 \rightarrow 2$  part of two particle  ${}_2GPD$  as:

$$\begin{aligned} \alpha_{[1]} \bar{D}_h^{AB}(x_1, x_2, Q_1, Q_2) &= \sum_{E, A', B'} \int_{Q_0^2}^{\min(Q_1^2, Q_2^2)} \frac{dk^2}{k^2} \frac{\alpha_s(k^2)}{2\pi} \int \frac{dy}{y} G_h^E(y; k^2) \\ &\times \int \frac{dz}{z(1-z)} V_E^{A'}(z) \frac{n_{A'} \alpha \bar{C}_{A'}^{B'}}{n_E} \\ &\times \alpha \bar{D}_{A'}^A\left(\frac{x_1}{zy}; Q_1^2, k^2\right) \alpha \bar{D}_{B'}^B\left(\frac{x_2}{(1-z)y}; Q_2^2, k^2\right). \end{aligned} \quad (31)$$

Using (8) and writing  $z_1 = \frac{x_1}{z_1 y}$ ,  $z_2 = \frac{x_2}{(1-z)y}$  this equation can be rewritten as:

$$\begin{aligned}
\alpha_{[1]} \bar{D}_h^{AB}(x_1, x_2, Q_1, Q_2) &= \sum_{E, A', B'} \int_{Q_0^2}^{\min(Q_1^2, Q_2^2)} \frac{dk^2}{k^2} \frac{\alpha_s(k^2)}{2\pi} \bar{S}_{A'}(k^2, Q_1) \bar{S}_{B'}(k^2, Q_2) \\
&\times \int_{x_1}^1 dz_1 \int_{x_2}^1 dz_2 \frac{x_1 x_2}{z_1^2 z_2^2 \left(\frac{x_1}{z_1} + \frac{x_2}{z_2}\right)} G_h^E\left(\frac{x_1}{z_1} + \frac{x_2}{z_2}; k^2\right) \\
&\times V_E^{A'}\left(\frac{x_1}{z_1 \left(\frac{x_1}{z_1} + \frac{x_2}{z_2}\right)}\right) \frac{n_{A'}}{n_E} \bar{C}_{A'}^{B'} \tilde{D}_{A'}^A(z_1; Q_1^2, k^2) \tilde{D}_{B'}^B(z_2; Q_2^2, k^2).
\end{aligned} \tag{32}$$

Here it's understood that  $G_h^E\left(\frac{x_1}{z_1} + \frac{x_2}{z_2}; k^2\right) = 0$  for  $\frac{x_1}{z_1} + \frac{x_2}{z_2} > 1$ . We have suppressed the representation index on the r.h.s although  $\bar{S}, \bar{C}$  and  $\tilde{D}$  are representation dependent. There is one problem with this equation, as can be seen from (16) and table II: for certain representations,  $\tilde{D} \propto \frac{1}{(1-z)^\lambda}$  with  $\lambda > 1$ . Therefore the integrals over  $z_{1,2}$  might diverge at the limit  $z_{1,2} \rightarrow 1$ . We delay the solution to this problem for section IID and for now assume these integrals are finite.

### *Self Consistency of the $\alpha_{[1]} \bar{D}_h^{AB}$ Normalization*

Equation (32) cannot be solved analytically, we delay its numerical solution to section III. We can solve it, however, in the approximation of no evolution. In this approximation, we neglect any  $k^2$  dependence of physical quantities. We call this approximation “0<sup>th</sup> order”. This approximation can also help us check the self consistency of the normalizations defined at (26). At this approximation

$$\alpha \bar{D}_A^B(x) \rightarrow \delta_A^B \delta(1-x), \tag{33}$$

Note the r.h.s is independent of  $\alpha$  since the representation affects only the evolution equation. we also set  $G_h^E(y; k^2) \rightarrow G_h^E(y)$  to be independent of  $k^2$ . We can now write (32) as (ignoring the  $k^2$  integral):

$$\alpha_{[1]} \bar{D}_h^{AB} = G_h^E(x_1 + x_2) \frac{V_E^A\left(\frac{x_1}{x_1+x_2}\right)}{x_1 + x_2} \frac{n_A}{n_E} \alpha \bar{C}_A^B. \tag{34}$$

Now there is no summation over  $B', A'$  and  $E$  is completely determined by charge conservation.

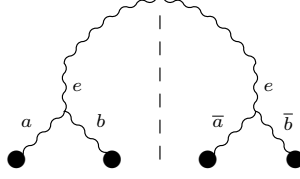


Figure 7. Diagram for the  $1 \rightarrow 2$  process and its complex conjugate where all particles are gluons,  $\bullet$  represents the hard process. The upper gluon connecting  $e$  is only symbolic of the color connection and does not represent an actual gluon.

On the other hand, we can compute  $[_1]D_{h;BC}^{a\bar{a}b\bar{b}}$ , which is defined by figure 5 to the same approximation. We first divide it to a momentum part which depends on the Bjorken variables  $x_1$  and  $x_2$  and a color part which depends on the color indices  $a, \bar{a}, b, \bar{b}$ :

$$[_1]D_{h;AB}^{a\bar{a}b\bar{b}}(x_1, x_2) = U_{h;AB}(x_1, x_2) \cdot T^{a\bar{a}b\bar{b}}. \quad (35)$$

The  $U$  factor describes a parton  $E$  originating from a hadron with Bjorken variable  $x_1 + x_2$  which then splits to  $A$  and  $B$  with Bjorken variables  $x_1$  and  $x_2$  respectively. It can therefore be written as:

$$U_{h;BC}(x_1, x_2) = G_h^E(x_1 + x_2) \frac{V_E^A\left(\frac{x_1}{x_1+x_2}\right)}{x_1 + x_2}. \quad (36)$$

Here  $G_h^E(x_1 + x_2)$  is the distribution of  $E$  in the hadron.  $V_E^A\left(\frac{x_1}{x_1+x_2}\right)$  is the splitting kernel from  $E$  to  $A$  ( $B$ ) with fraction of longitudinal momentum  $\frac{x_1}{x_1+x_2}$  ( $\frac{x_2}{x_1+x_2}$ ) compared to  $E$ . The division by  $\frac{1}{x_1+x_2}$  comes from the fact that  $E$  has actually a Bjorken variable of  $x_1 + x_2$  and not 1 as assumed when computing  $V_A^B$  in table I. The color factor  $T^{a\bar{a}b\bar{b}}$  depend on the type of particles (gluons or fermions). For example assume  $A = B = G$  ( $A$  and  $B$  are gluons) which then means  $E = G$  also (by charge conservation) so the diagram in figure 7 has the color factor of:

$$T^{a\bar{a}b\bar{b}} = f^{eab} f^{e\bar{a}\bar{b}} = \sum_{\alpha} c_{\alpha} P_{a\bar{a}b\bar{b}}^{\alpha}. \quad (37)$$

Here  $c_{\alpha}$  are given by the contraction identity (Appendix E)  $c_{\alpha} = \alpha \bar{C}_G^G = \{\frac{N}{2}, 0, N, \frac{N}{2}, -1, 1\}$  so we can write the whole distribution as:

$${}_{[1]}D_{h;GG}^{a\bar{a}b\bar{b}}(x_1, x_2) = G_h^G(x_1 + x_2) \frac{V_G^G\left(\frac{x_1}{x_1+x_2}\right)}{x_1 + x_2} \sum_{\alpha} \alpha \bar{C}_G^G P_{a\bar{a}b\bar{b}}^{\alpha} = \sum_{\alpha} \alpha {}_{[1]}\bar{D}_h^{GG} P_{a\bar{a}b\bar{b}}^{\alpha}. \quad (38)$$

Where in the last step we used (34), those proving (27) for the 0th order case and seeing the normalizations are all correct. Equation (34) has another interesting property: we see that for certain representations  $\alpha {}_{[1]}\bar{D}_h^{AB}$  should be negative. This is not really a surprise as non singlet or spin dependent distributions can, in general, be negative [17] and only the observable cross section, after considering all color channels, should be positive.

Let us recall that we need  $1 \rightarrow 2$   ${}_2GPD$  only at  $\vec{\Delta} = 0$ , since in our total cross section this  ${}_2GPD$  is convoluted with nonperturbative two gluon form factors from the second nucleon, that decrease in  $\Delta$  much more rapidly than the perturbative  $1 \rightarrow 2$  piece [7, 9].

#### D. Regularization of $z_i \rightarrow 1$ Singularity

As we have seen before the functions  $\bar{D}_B^A(z, Q^2, k_0^2)$  are the building blocks for the  $1 \rightarrow 2$  part of the  ${}_2GPD$ , corresponding to upper parts of the Feynman diagrams of figs. 1-3. Note that  $z$  dependence is fully contained in  $\tilde{D}_B^A(z, Q^2, k_0^2)$  since  $\alpha \bar{S}_A$  do not depend in  $z$ . Although we can calculate  $\tilde{D}_B^A(z, Q^2, k_0^2)$  numerically their asymptotics at  $z \rightarrow 1$  was found analytically, see eq. (16). It has a form  $1/(1-z)^{1-g}$ , where  $g$  is proportional to running coupling constant, and is  $g > 0$  for singlet case, so the integral (32) converges in the  $z_1 \rightarrow 1$  and  $z_2 \rightarrow 1$  limit. However for the nonsinglet case  $g \sim \xi \bar{C}_A^A$  can be negative, since the colour factors  $\bar{C}_A^A$  are negative. We assume that after integration over  $z$  ( $z_1, z_2$ ) the resulting function is an analytic function of  $g$  (i.e. of running coupling constant). Then the theory of generalised functions [33, 34] guarantees the unique analytical continuation into  $g < 0$  domain. Note that it is possible to calculate  ${}_2GPD$  also by solving numerically the evolution equation. In this way one can indeed avoid dealing with singularities in nonsinglet fundamental solutions. Proof of equivalence of both approaches is given in Appendix F.

The analytical continuation method was already used in connection with diverging integrals in  $z$  for observables related to Double Drell Yan in [11], see also [35] for detailed discussion.

Let us address the issue of divergent untegrals in more detail, since the analytical continuation in  $g$  was explicitly considered in [11, 33, 35] only for one-dimensional integrals.

In the 1-dimensional case, such integrals can be made finite in the following way. Consider a function  $f(z)$  that is bounded in the segment  $[0, 1]$  and smooth in some neighborhood of 0. We

then define the integral

$$\int_0^1 dx \frac{f(x)}{x^\lambda} := \int_0^1 \frac{f(x) - f(0)}{x^\lambda} dx + \frac{f(0)}{1-\lambda} \quad (39)$$

for every  $\lambda < 2$  except  $\lambda = 1, 0$ . For  $\lambda < 1$  this relation clearly holds as both the l.h.s and the r.h.s integrals converge. For  $1 < \lambda < 2$  the l.h.s formally diverges but the r.h.s converges and is the analytical continuation of the l.h.s as a function of the complex variable  $\lambda$ . We'll now generalize this method to 2 dimensional functions. Let  $F(z_1, z_2)$  be a function that is well defined and bounded in the region  $(z_1, z_2) \in [x_1, 1] \times [x_2, 1]$  for  $0 < x_1, x_2 < 1$ . And also has a finite derivative at the lines  $z_1 = 1$  and  $z_2 = 1$ . Note that we do not require  $F$  to be continuous except at these lines. Then look at the integral

$$I = \int_{x_1}^1 dz_1 \int_{x_2}^1 dz_2 \frac{F(z_1, z_2)}{(1-z_1)^{1-g_1} (1-z_2)^{1-g_2}} \quad (40)$$

for  $g_1, g_2 > 0$  this integral is well defined and can be written as a sum of four integrals:

$$I := I_A + I_B + I_C + I_D, \quad (41a)$$

$$I_A = \int_{x_1}^1 dz_1 \int_{x_2}^1 dz_2 \frac{F(z_1, z_2) - F(1, z_2) - F(z_1, 1) + F(1, 1)}{(1-z_1)^{1-g_1} (1-z_2)^{1-g_2}}, \quad (41b)$$

$$I_B = \int_{x_1}^1 dz_1 \int_{x_2}^1 dz_2 \frac{F(z_1, 1) - F(1, 1)}{(1-z_1)^{1-g_1} (1-z_2)^{1-g_2}} = \frac{(1-x_2)^{g_2}}{g_2} \int_{x_1}^1 dz_1 \frac{F(z_1, 1) - F(1, 1)}{(1-z_1)^{1-g_1}}, \quad (41c)$$

$$I_C = \int_{x_1}^1 dz_1 \int_{x_2}^1 dz_2 \frac{F(1, z_2) - F(1, 1)}{(1-z_1)^{1-g_1} (1-z_2)^{1-g_2}} = \frac{(1-x_1)^{g_1}}{g_1} \int_{x_2}^1 dz_2 \frac{F(1, z_2) - F(1, 1)}{(1-z_2)^{1-g_2}}, \quad (41d)$$

$$I_D = \int_{x_1}^1 dz_1 \int_{x_2}^1 dz_2 \frac{F(1, 1)}{(1-z_1)^{1-g_1} (1-z_2)^{1-g_2}} = \frac{(1-x_2)^{g_2} (1-x_1)^{g_1}}{g_2 g_1} F(1, 1). \quad (41e)$$

We now analytically continue  $I_A, I_B, I_C$  and  $I_D$  as functions of  $g_1, g_2$  to the region  $-1 < g_1, g_2 < 0$ . The integrals on the r.h.s still converge because of the condition that  $\partial_{z_i} F|_{z_i=1}$  exist. Therefore  $I$  is well defined and finite in this region too, even when the r.h.s of (40) formally diverges. In our case, we can define:

$$\begin{aligned}
F(z_1, z_2) &= \frac{x_1 x_2}{z_1^2 z_2^2 \left( \frac{x_1}{z_1} + \frac{x_2}{z_2} \right)} G_h^E \left( \frac{x_1}{z_1} + \frac{x_2}{z_2}; k^2 \right) V_E^{A'} \left( \frac{x_1}{z_1 \left( \frac{x_1}{z_1} + \frac{x_2}{z_2} \right)} \right) \\
&\times \frac{n_{A'} \alpha \bar{C}_{A'}^{B'} \tilde{D}_{A'}^A(z_1; Q_1^2, k^2) \tilde{D}_{B'}^B(z_2; Q_2^2, k^2)}{n_E (1-z_1)^{g_1-1} (1-z_2)^{g_2-1}},
\end{aligned} \tag{42a}$$

$$g_1 = 4\xi(Q_1, k) \bar{C}_{A'}^A, \tag{42b}$$

$$g_2 = 4\xi(Q_2, k) \bar{C}_{B'}^B. \tag{42c}$$

These quantities satisfy the rules above due to (16) as long as

$$4\xi \bar{C}_G^G, 4\xi \bar{C}_F^F < -1, \tag{43a}$$

$$4\xi \bar{C}_F^G - 1 < 4\xi \bar{C}_F^F, \tag{43b}$$

$$4\xi \bar{C}_G^F - 1 < 4\xi \bar{C}_G^G. \tag{43c}$$

For the values given in table II, these conditions are fulfilled for  $\xi < 0.2$  (in our choice of  $Q_0$  this condition is equivalent to  $k \approx 200 \text{ GeV}$ ). This procedure gives a regularization for the integrals in (32), which we'll implement in the numerical calculation. For higher values of  $k$  one can use a second order version of this regularization (for which the  $1d$  case is given in [33, 34]) but we'll not need that in this paper.

### III. NUMERICS

In this section, we'll use the results of the previous chapters to give numeric evaluation of the non-singlet channels distributions relative to the singlet channel distributions. We'll use (32) to

compute  $\alpha_{[1]} \overline{D}_h^{AB}$ . However, it'll be more instructive to actually investigate

$$R^\alpha := \frac{7}{3} \frac{\alpha_{[1]} \overline{D}^{GG}}{GGGG}, \quad (44)$$

which is analogous to  $R$  used in [9] and directly enters the cross section.

In order to make the computation we need first to express all the components of (32) in a way that can be numerically computable.  $\alpha \overline{S}_A$  can be computed numerically using (9) and the regularization (7).  $\tilde{D}$  that were defined by (8) have no close expression to use but we explained in section II A how they can be numerically evaluated. For  $G^A$  the single parton distribution we use the expressions given in [31] and we remember to take the  $z_1$  and  $z_2$  integrals in (32) according to the prescription given in section II D.

Eq. (32) has an interesting property: since the lower momentum in the suppression factor  $\overline{S}$  is  $k^2$  and not  $Q_0^2$ , and  $k^2$  ranges all the way up to  $Q^2 = \min(Q_1^2, Q_2^2)$ , the phase space gets larger for larger  $Q^2$ . So we expect  $\left| \alpha_{[1]} \overline{D}_h^{CB} \right|$  to moderately grow with  $Q$ , this statement is in direct contrast to the regular color non-singlet  $2 \rightarrow 2$  process (as explained in section II B) which should strongly decrease with the increasing  $Q$  [12, 13]. Moreover, when  $Q_1 \approx Q_2 \approx Q$ , there is always a region at  $k \sim Q$  for which the suppression factor  $\overline{S}(k^2, Q_1^2) \overline{S}(k^2, Q_2^2)$  is not significant, even when  $Q$  is very large.

We consider the kinematics where the scattering angle in the c.m. in each hard process is  $\pi/2$ . We work with leading logarithmic accuracy, so we take  $p_T \sim Q$ , where  $p_T$  is the transverse momenta of the final states hard partons. Then we have in our kinematics

$$x = \sqrt{\frac{4p_T^2}{s}} \sim \sqrt{\frac{4Q^2}{s}}, \quad (45)$$

see [36] for the details of kinematics in 2 to 2 hard collisions. Where  $s$  is the center of mass energy of the hadron collision. We'll check the contribution of non singlet color channels at several different kinematics:

- At LHC where  $s = 1.96 \times 10^8$  [ $GeV^2$ ]
- At the Tevatron where  $s = 4 \cdot 10^6$  [ $GeV^2$ ]
- And at even lower hadron energy where  $s = 1 \cdot 10^5$  [ $GeV^2$ ]. We look at this energy scale because we expect the contributions to be relatively high in this region, but there might not be enough DPS processes to measure it in experiments.

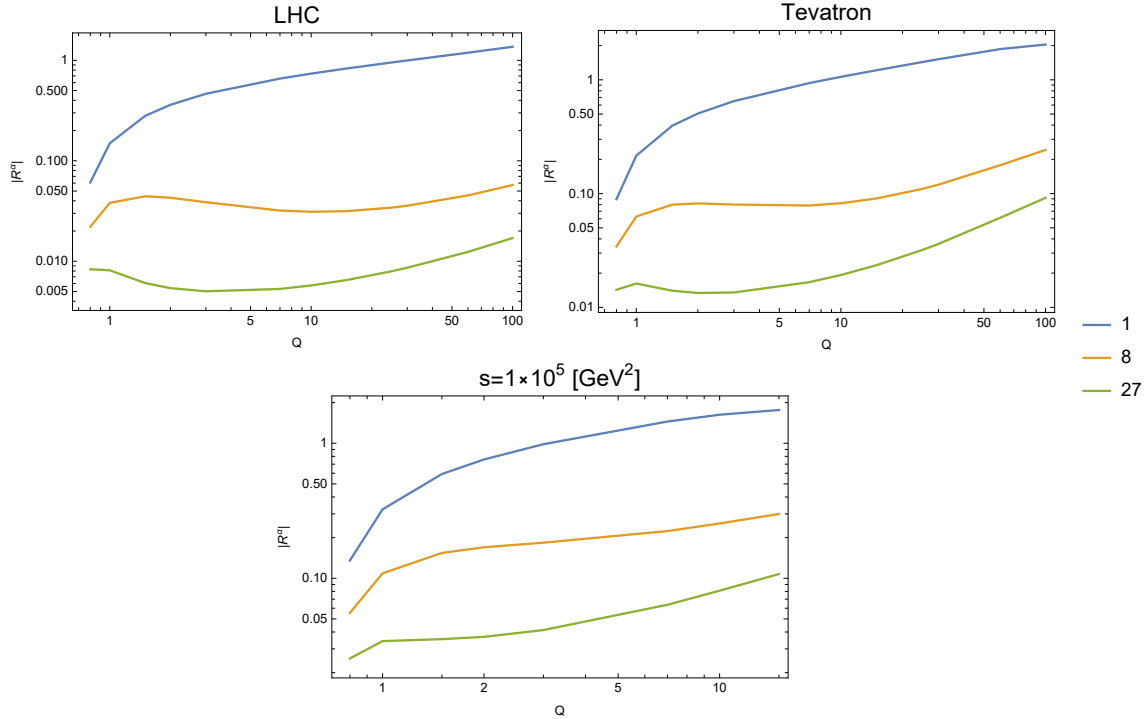


Figure 8. Absolute values of  $R^\alpha$  ( $R^{27}$  is negative, the others are strictly positive) at LHC, Tevatron and  $s = 1 \cdot 10^5$  [GeV<sup>2</sup>] kinematics for  $Q_1^2 = Q_2^2 = Q^2$ ,  $x_1 = x_2 = x$  and  $N = 3$ . The values of  $R^{8_a}$  and  $R^{8_s}$  are very similar and therefore only  $R^{8_a}$  is shown on the graph. The plot is logarithmic in both axes.

We expect the non-singlet contributions to be largest especially when the two different hard processes are at similar scales, i.e.  $Q_1^2 = Q_2^2 := Q^2$  and  $x_1 = x_2 = x_3 = x_4 := x$ . At these scales, the values of the  $R^\alpha$  (which are  $\alpha_{[1]} \overline{D}_h^{GG}$  normalized by  $\frac{7}{3} \cdot \frac{1}{[G_p^G]^2}$  as explained in (44)) are shown in figure 8 as a function of  $Q$ .

We see that the singlet distribution is much larger than the octet and 27 representation. But we also see that the non-singlet distribution values stay the same and even slowly increase at high energy (as predicted). This behavior is unlike what is expected from the non-singlet DPDs that should be highly suppressed at high energies [12, 13]. The source of the seen minimum value of the non-singlet functions is due to the normalization,  $G_p^G(x, Q^2)$  as a function of  $Q$  (where we take  $x = \sqrt{\frac{4 \cdot Q^2}{s}}$ ).

It's also interesting to look at the  $k$  behavior of the integrand of (32) to explicitly see which splitting scales contribute the most to  $\alpha_{[1]} \overline{D}_h^{GG}$ . The value of this integrand (after performing the  $z_1$  and  $z_2$  integrals) is shown on the left of figure 9 for the LHC kinematics and  $Q = 50$  [GeV]



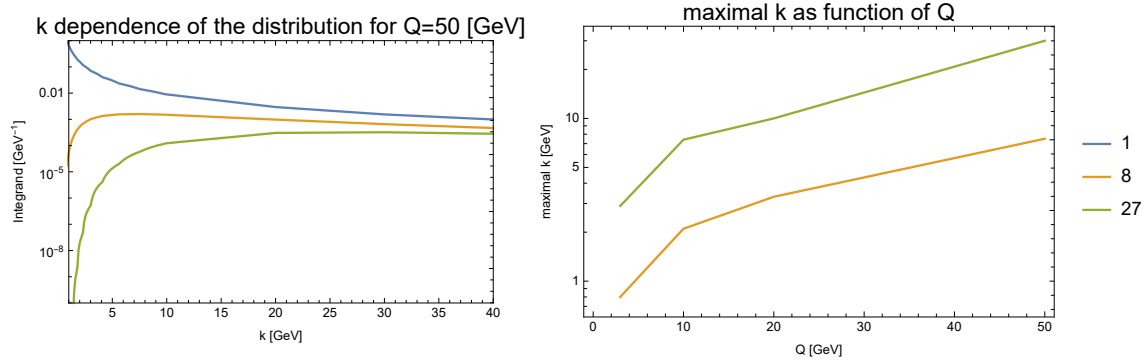


Figure 9. On the left: the integrand of (32), after performing the  $z_1$  and  $z_2$  integrals, in the LHC kinematics and  $Q = 50$  [GeV] for different representations and values of  $k$ . On the right: The value of  $k$  for which the maximal value of this integrand is obtained as a function of  $Q$ .

(similar behavior is also seen for different kinematics). It can be seen from this figure that the singlet distribution gets most of the contribution from the low  $k$  region. In contrast, the non singlet distributions are suppressed at low  $k$  and get notable contributions only starting at  $k > 5$  [GeV]. The  $k$  for which the maximal value of the integrand is obtained is shown in figure 9 on the right for different values of  $Q$  at the LHC kinematics. As is expected the dominant splitting scale increases with  $Q$ .

#### IV. CONCLUSION

In this paper, we studied the the color correlations in the nucleon. We have considered for simplicity the case of symmetric kinematics, when  $x_1 = x_2 = x_3 = x_4 = x$  and  $Q_1 = Q_2 = Q$ .

We have seen that it is possible to avoid the conventional Sudakov suppression of color correlations, by considering specific  $1 \rightarrow 2$  processes depicted in figure 2. The reason is the increase of the split scale with the increase of the hard scale, in difference to the singlet case.

Although these contributions do not decrease with the increase of the transverse scale, they are still small due to relative smallness of the color factors relative to the singlet case.

We saw that in the Tevatron and LHC kinematics they amount to about 1-10% of the singlet  $1 \rightarrow 2$  distribution.

The color correlation contribution increases if we go to smaller energies, however, we must remember that for smaller energies there might be not enough statistics to observe DPS.

Nevertheless, the fact that perturbative color correlations do not decrease with transverse scale makes it potentially possible to observe them and thus have further insight into the precise QCD description of the nucleon wave functions.

One possibility to observe the color correlations contributions due to  $1 \rightarrow 2$  processes discussed here is the so called  $1v1$  processes, with two  $1 \rightarrow 2$  processes from the side of each colliding nucleons. These processes were considered recently in [19], although further work may be needed to distinguish this particular contribution in the process cross section.

### ACKNOWLEDGMENTS

We thank Yu Dokshitzer and M. Strikman for useful discussions and M. Strikman for reading the article. This research was supported by ISF grant 2025311 and BSF grant 2020115.

### Appendix A: Color Kernels

We now turn to compute explicitly the factors  ${}^\alpha \overline{C}_A^B$  for different representations. These factors were derived partially in [11] for polarized particles and completely in [15]. In this section we rederive them in our formalism for completeness. Let it be remind that for the singlet representation (as in the original DGLAP case), these factors are shown in table III.

R	1
$C_F^F$	$\frac{N^2-1}{2N}$
$C_F^G$	$\frac{N^2-1}{2N}$
$C_G^F$	$\frac{1}{2}$
$C_G^G$	$N$

Table III. Color factors for the singlet representation

We start by considering the simplest case of  $R = 27$ ,  $q\bar{q}$  cannot be in this representation, and therefore  ${}^{27}\overline{C}_F^F = {}^{27}\overline{C}_F^G = {}^{27}\overline{C}_F^G = 0$ . In order to find the only non-zero kernel  ${}^{27}\overline{C}_G^G$  attach the 27 projector to a gluon ladder, as shown in fig. 10. The color factor for such a diagram is well known [40, 41] and equal to  ${}^{27}\overline{C}_G^G = -1$ . This result is a special case of the ‘‘interaction force identity’’, as will be explained in Appendix E.

By the same line of argument  ${}^{10}\overline{C}_F^F = {}^{10}\overline{C}_G^F = {}^{10}\overline{C}_F^G = {}^{10}\overline{C}_G^G = 0$  where 10 is the sum of the irreducible decouple representations [41], we, therefore, conclude that the representation 10 does

$$\text{Diagram} = \bar{C}_G^G(27) \times P_{27}$$

Figure 10. The ladder diagram that determines  $\bar{C}_G^G(27)$ ,  $P^{27}$  is the 2 gluon projector to the irreducible representation 27.

not evolve in ladders and should not contribute to physical processes. We now turn to consider the octet representation of quarks and the symmetric octet ( $8_s$ ) and anti-symmetric octet ( $8_a$ ) of gluons. Considering these representations raises two problems that were absent when we considered the 27 and 10 representations:

- There is now a mixing of quark and gluons, this poses a certain ambiguity to the  $\bar{C}_G^F$ ,  $\bar{C}_F^G$  kernels.
- The second problem is that the single quark octet representation mixes with the two gluon octet representations. This effect potentially could make  $\bar{C}_F^G$  a matrix connecting two representations rather than a simple factor, which would ruin the analysis made in section II A.

We'll delay the solution of the first problem to the end of this section, and until then keep the freedom of normalization of these kernels. As for the second problem, luckily it can be solved easily. This solution is done by considering, instead of quark or anti-quark ladders separately, the sum of quark and anti quark ladders, as shown in fig. 11. This solution, although very elegant, works only as long as there is symmetry between quarks and anti-quarks. When such symmetry breaks (for example when considering the valence parton distribution) it will no longer work. In this paper, we consider kinematic regions where valence distribution is small compared to gluon or sea distributions.

### 1. Color Factor for the $8_a$ Representation

We start by concretely looking at the  $8_a$  representation. Consider the two structures  $G_a$  and  $Q_a$  that represent this representation for quarks and gluons, as shown in fig 12. We'll show that these structures propagate within the ladder and do not mix with any other structures. The color

$$\begin{aligned}
& \left. \begin{array}{c} \left. \begin{array}{c} a \\ \text{---} \\ c \end{array} \right\} \\ \text{---} \\ \left. \begin{array}{c} b \\ \text{---} \\ d \end{array} \right\} \end{array} \right\} = f^{aec} f^{bde} = V_{ab;cd} \quad (a) \\
& \left. \begin{array}{c} \left. \begin{array}{c} a \\ \text{---} \\ i \end{array} \right\} \\ \text{---} \\ \left. \begin{array}{c} b \\ \text{---} \\ j \end{array} \right\} \end{array} \right\} + \left. \begin{array}{c} \left. \begin{array}{c} a \\ \text{---} \\ i \end{array} \right\} \\ \text{---} \\ \left. \begin{array}{c} b \\ \text{---} \\ j \end{array} \right\} \end{array} \right\} = t_{ik}^a t_{kj}^b + t_{jk}^b t_{ki}^a \quad (b) \\
& \left. \begin{array}{c} \left. \begin{array}{c} i \\ \text{---} \\ c \end{array} \right\} \\ \text{---} \\ \left. \begin{array}{c} j \\ \text{---} \\ d \end{array} \right\} \end{array} \right\} + \left. \begin{array}{c} \left. \begin{array}{c} i \\ \text{---} \\ c \end{array} \right\} \\ \text{---} \\ \left. \begin{array}{c} j \\ \text{---} \\ d \end{array} \right\} \end{array} \right\} = t_{jk}^d t_{ki}^c + t_{ik}^c t_{kj}^d \quad (c) \\
& \left. \begin{array}{c} \left. \begin{array}{c} i \\ \text{---} \\ m \end{array} \right\} \\ \text{---} \\ \left. \begin{array}{c} j \\ \text{---} \\ n \end{array} \right\} \end{array} \right\} + \left. \begin{array}{c} \left. \begin{array}{c} i \\ \text{---} \\ m \end{array} \right\} \\ \text{---} \\ \left. \begin{array}{c} j \\ \text{---} \\ n \end{array} \right\} \end{array} \right\} = t_{mi}^e t_{jn}^e + t_{im}^e t_{nj}^e \quad (d)
\end{aligned}$$

Figure 11. The DGLAP ladders associated with  $\overline{C}_G^G$  (a),  $\overline{C}_G^F$  (b),  $\overline{C}_F^G$  (c) and  $\overline{C}_F^F$  (d), where we have summed quark and anti-quark ladders together.

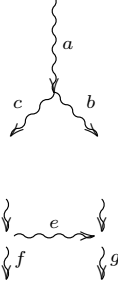
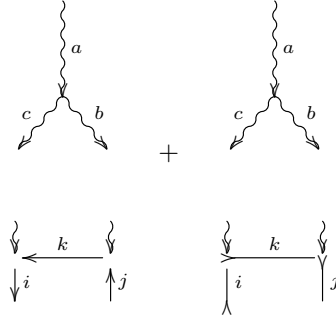
$$\begin{aligned}
& \alpha \cdot \left. \begin{array}{c} e \\ \text{---} \\ \left. \begin{array}{c} c \\ \text{---} \\ d \end{array} \right\} \end{array} \right\} \quad G_a^{dc} = i\alpha f^{dce} \quad (a) \\
& \beta \cdot \left. \begin{array}{c} e \\ \text{---} \\ \left. \begin{array}{c} k \\ \text{---} \\ l \end{array} \right\} \end{array} \right\} - \left. \begin{array}{c} e \\ \text{---} \\ \left. \begin{array}{c} k \\ \text{---} \\ l \end{array} \right\} \end{array} \right\} \quad Q_a^{kl} = \beta (t_{kl}^e - t_{lk}^e) \quad (b)
\end{aligned}$$

Figure 12. The anti-symmetric octet ( $8_a$ ) structures  $G_a$  (a) and  $Q_a$  (b).  $\alpha$  and  $\beta$  are arbitrary real numbers.

kernels for  $8_a$  will be the contractions of these structures with the ladders given in figure 11.

$$a. \quad \overline{C}_G^G$$

We now contract the ladder of type  $\Phi_G^G$  with the color structure  $G$  as seen in figure 13:

Figure 13. Contraction of  $\Phi_G^G$  with  $G_a$ Figure 14. Contraction of  $\Phi_F^G$  with  $G_a$ 

$$G_a^{bc} \cdot V_{bc;gf} = i\alpha f^{bca} (c_\alpha P_{bc;gf}^\alpha). \quad (\text{A1})$$

We use the contraction property of the projectors (the generalized version as proved in section E) to cancel every projector but  $\delta_a$  and are left with:

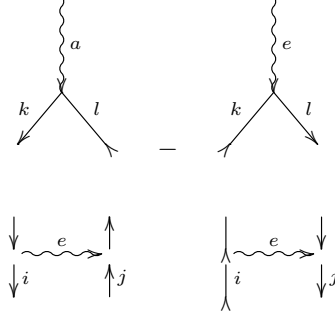
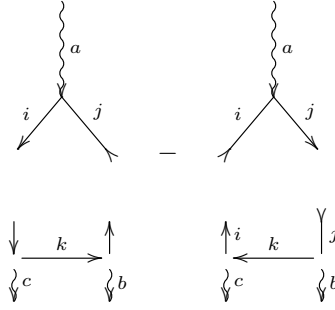
$$= i\alpha f^{bca} c_{\delta_a} P_{bc;gf}^{\delta_a} = i\alpha c_{\delta_a} \left( f^{bca} \frac{f^{bce} f g f e}{N} \right) = c_{\delta_a} \left( \alpha i N \frac{f g f a}{N} \right) = c_{\delta_a} G_{gf}.$$

Here, as we'll see in Appendix E,  $c_{\delta_a} = \frac{N}{2}$ .

b.  $\overline{C}_F^G$

This contraction is shown in figure 14 and is written as:

$$i\alpha f^{bca} \left( t_{ik}^c t_{kj}^b + t_{jk}^b t_{ki}^c \right) = -\alpha i f^{cba} t_{ik}^c t_{kj}^b + i f^{bca} t_{jk}^b t_{ki}^c = \alpha \frac{N}{2} (t_{ij}^e - t_{ji}^e) = \frac{\alpha N}{\beta 2} Q_{ij}. \quad (\text{A2})$$

Figure 15. Contraction of  $\Phi_F^F$  with  $Q_a$ Figure 16. Contraction of  $\Phi_G^F$  with  $Q_a$ 

So we get that  $\overline{C}_F^G = \frac{\alpha}{\beta} \frac{N}{2}$ .

c.  $\overline{C}_F^F$

This contraction is viewed on figure 15 and is written as:

$$\begin{aligned} Q_a^{ij} (t_{ik}^e t_{lj}^e + t_{ki}^e t_{jl}^e) &= \beta (t_{kl}^a t_{ik}^e t_{lj}^e - t_{lk}^a t_{ki}^e t_{jl}^e) = \beta (t_{ik}^e t_{kl}^a t_{lj}^e - t_{jl}^e t_{lk}^a t_{ki}^e) \\ &= -\beta \frac{1}{2N} (t_{ij}^a - t_{ji}^a) = -\frac{1}{2N} Q_{ij}. \end{aligned} \quad (\text{A3})$$

So the factor is  $\overline{C}_F^F = -\frac{1}{2N}$ .

d.  $\overline{C}_G^F$

This contraction is viewed on figure 16 and is written as

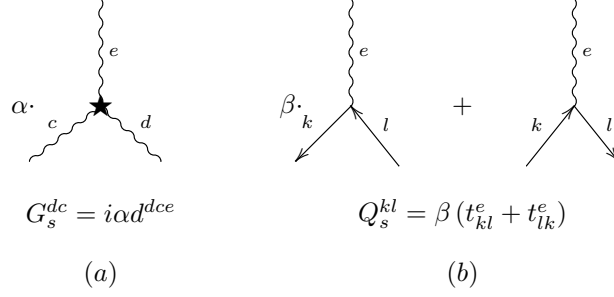


Figure 17. The symmetric octet ( $8_s$ ) structures  $G_s$  (a) and  $Q_s$  (b).  $\alpha$  and  $\beta$  are arbitrary real numbers that are not necessarily the same as for  $8_a$ .

$$\begin{aligned}
Q_a^{ij} \left( t_{jk}^b t_{ki}^c + t_{ik}^c t_{kj}^b \right) &= \beta \left( t_{ij}^a t_{jk}^b t_{ki}^c - t_{ji}^a t_{ik}^c t_{kj}^b \right) \\
&= \beta \left( \text{tr} \left[ t^a t^b t^c \right] - \text{tr} \left[ t^a t^c t^b \right] \right) \\
&= \beta \frac{1}{4} \left( i f^{abc} + d^{abc} - i f^{acb} - d^{acb} \right) \\
&= \beta \frac{i}{4} \left( f^{abc} - f^{acb} \right) \\
&= \beta \frac{i}{2} f^{bca} \\
&= \frac{\beta}{\alpha} \frac{1}{2} G_{bc}.
\end{aligned} \tag{A4}$$

So the factor is  $\overline{C}_G^F = \frac{\beta}{\alpha} \frac{1}{2}$ .

## 2. Color Factor for the $8_s$ Representation

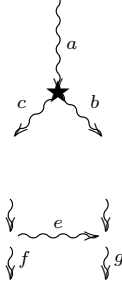
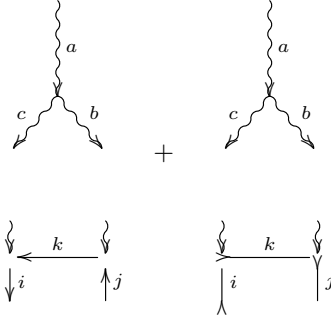
We now look at the  $8_s$  representation. Consider two new structures  $G_s$  and  $Q_s$  that represent this representation for gluon and quark, as shown in fig 17. The rest of the analysis is the same.

a.  $\overline{C}_G^G$

We now contract the ladder of type  $\Phi_G^G$  with the color structure  $G_s$  as seen in figure 18:

$$G_s^{bc} \cdot V_{bc;gf} = \alpha d^{bca} \left( c_\alpha P_{bc;gf}^\alpha \right). \tag{A5}$$

We use the contraction property of the projectors (the generalized version) to cancel every projector but  $8_s$  and are left with:

Figure 18. Contraction of  $\Phi_G^G$  with  $G_s$ Figure 19. Contraction of  $\Phi_F^G$  with  $G_s$ 

$$= \alpha d^{bca} c_{8_s} P_{bc;gf}^{8_s} = \alpha c_{8_s} \left( d^{bca} d^{bce} d^{gfe} \frac{N}{N^2 - 4} \right) = c_{8_s} \left( \alpha \frac{N^2 - 4}{N} d^{gfa} \frac{N}{N^2 - 4} \right) = c_{8_s} G_{gf}^s.$$

Where, as we have seen  $c_{8_s} = \frac{N}{2}$ .

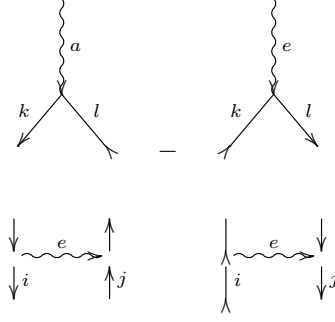
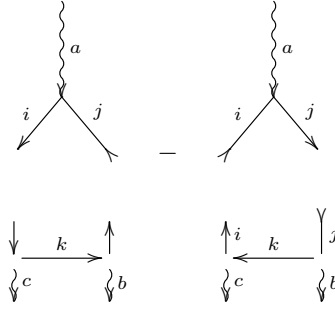
b.  $\bar{C}_F^G$

This contraction is shown in figure 19 and is written as:

$$\alpha d^{bca} \left( t_{ik}^c t_{kj}^b + t_{jk}^b t_{ki}^c \right) = \alpha \left( d^{cba} t_{ik}^c t_{kj}^b + d^{bca} t_{jk}^b t_{ki}^c \right) = \alpha \frac{N^2 - 4}{2N} (t_{ij}^e + t_{ji}^e) = \frac{\alpha}{\beta} \frac{N^2 - 4}{2N} Q_{ij}^s. \quad (\text{A6})$$

So we get that  $\bar{C}_F^G = \frac{N^2 - 4}{2N}$ .



Figure 20. Contraction of  $\Phi_F^F$  with  $Q_s$ Figure 21. Contraction of  $\Phi_G^F$  with  $Q_s$ 

$$c. \quad \overline{C}_F^F$$

This contraction is viewed on figure 20 and is written as:

$$\begin{aligned}
 Q_s^{ij} (t_{ik}^e t_{lj}^e + t_{ki}^e t_{jl}^e) &= \beta (t_{kl}^a t_{ik}^e t_{lj}^e + t_{lk}^a t_{ki}^e t_{jl}^e) \\
 &= \beta (t_{ik}^e t_{kl}^a t_{lj}^e + t_{jl}^e t_{lk}^a t_{ki}^e) \\
 &= -\frac{\beta}{2N} (t_{ij}^a + t_{ji}^a) = -\frac{1}{2N} Q_{ij}^s.
 \end{aligned} \tag{A7}$$

So the factor is  $\overline{C}_F^F = -\frac{1}{2N}$ .

$$d. \quad \overline{C}_G^F$$

This contraction is viewed on figure 21 and is written as

$$\begin{aligned}
Q_s^{ij} \left( t_{jk}^b t_{ki}^c + t_{ik}^c t_{kj}^b \right) &= \beta \left( t_{ij}^a t_{jk}^b t_{ki}^c + t_{ji}^a t_{ik}^c t_{kj}^b \right) = \\
&= \beta \left( \text{tr} \left[ t^a t^b t^c \right] + \text{tr} \left[ t^a t^c t^b \right] \right) \\
&= \beta \frac{1}{4} \left( i f^{abc} + d^{abc} + i f^{acb} + d^{acb} \right) \\
&= \beta \frac{i}{4} \left( d^{abc} + d^{acb} \right) \\
&= \beta \frac{1}{2} d^{abc} \\
&= \frac{\beta}{\alpha} \frac{1}{2} G_{bc}^s
\end{aligned} \tag{A8}$$

So the factor is  $\overline{C}_G^F = \frac{\beta}{\alpha} \frac{1}{2} G_{bc}^s$ .

### 3. Normalization of $\overline{C}_F^G$ and $\overline{C}_G^F$

Note that the color factors given above for  $\overline{C}_F^G$  and  $\overline{C}_G^F$  are not well defined and depend on the ratio of  $\frac{\alpha}{\beta}$  which was arbitrary. Therefore only the multiplication  $C_G^F \cdot C_F^G$  is well defined. In order to derive well defined color factors we impose the condition that a ladder would be well defined independently of whether we go from quark to gluon or from gluon to quark as shown in figure 22.

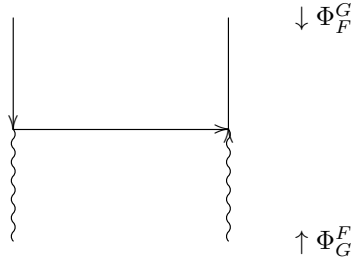


Figure 22. gluon to quark ladder diagram.

In our convention the ladder end in the hard process and therefore we sum over the color (and flavor) indices of the final (superscript) parton type and average over the color (and flavor) indices of the initial (subscript) parton type. This convention means that if we take the diagram in figure 22 from above or from below it will be equal only if we compensate for the averaging of the initial parton (and therefore effectively summing for both initial and final parton color and flavor indices):

$$\underbrace{N}_{\text{"types" of quarks}} \bar{\Phi}_F^G = \underbrace{(N^2 - 1)}_{\text{"types" of gluons}} \bar{\Phi}_G^F. \quad (\text{A9})$$

The  $z$  part of this argument is true[21] so we'll ignore it and get for the color-flavor part:

$$N \bar{C}_F^G = (N^2 - 1) \bar{C}_G^F, \quad (\text{A10})$$

$$\frac{\bar{C}_F^G}{\bar{C}_G^F} = \frac{N^2 - 1}{N}. \quad (\text{A11})$$

Note that this equation is actually independent of the color channel and therefore should be true for both the singlet and octet channels. Indeed for the singlet channel we have:

$$\frac{\bar{C}_F^G}{\bar{C}_G^F} = \frac{\frac{N^2-1}{2N}}{\frac{1}{2}} = \frac{N^2 - 1}{N}. \quad (\text{A12})$$

a.  $8_a$

Now the color factor multiplication is  $\bar{C}_F^G \bar{C}_G^F = \frac{N}{4}$ , therefore we can solve:

$$8_a \bar{C}_G^F = \frac{1}{2} \sqrt{\frac{N^2}{2(N^2 - 1)}}, \quad (\text{A13a})$$

$$8_a \bar{C}_F^G = \sqrt{\frac{N^2 - 1}{8}}. \quad (\text{A13b})$$

b.  $8_s$

Now the color factor multiplication is  $\bar{C}_F^G \bar{C}_G^F = \frac{N^2 - 4}{4N^2}$ , therefore we can solve:

$$8_s \bar{C}_G^F = \frac{1}{2} \sqrt{\frac{N^2 - 4}{2(N^2 - 1)}}, \quad (\text{A14a})$$

$$8_s \bar{C}_F^G = \frac{1}{2N} \sqrt{\frac{(N^2 - 4)(N^2 - 1)}{2}}. \quad (\text{A14b})$$

## Appendix B: Formal Derivation of the Non-Singlet DGLAP Equation

In this section, we give a more detailed and formal derivation of (5). We start with the Bethe-Salpeter equation for  $D_A^B$ , the singlet structure function, that comes from considering ladder type diagrams [21]:

$$D_A^B(x, Q^2) = \delta_A^B (1-x) d_A(k_0^2) d_B^{-1}(Q^2) + d_B^{-1}(Q^2) \sum_C \int_{zk_0^2}^{Q^2} \frac{dk^2}{k^2} \int_0^1 \frac{dz}{z} A_A^C d_B(k^2) \Phi_C^B(z) D_A^C\left(\frac{x}{z}, k^2\right). \quad (\text{B1})$$

Here:

- $d_A$  is the renormalization of particle  $A$ .
- $A_A^C = d_A\left(\frac{k^2}{z}\right) d_C(k^2) d_G \Gamma^2$  is the renormalization of the ladder, which we take to be  $\frac{\alpha(k^2)}{4\pi}$ .
- $\Phi_A^C(z) = C_A^B \cdot V(z)$  is the singlet splitting function as explained in the text.
- $A, B, C$  are types of partons, e.g gluon, quark, anti-quark.

$d_A$  obeys the relation [21]:

$$\frac{\partial}{\partial \ln(Q^2)} d_B(Q^2) = d_B(Q^2) \sum_C \int_0^1 z \frac{\alpha(Q^2)}{4\pi} \Phi_C^B(z) dz. \quad (\text{B2})$$

This equation represents virtual corrections of the parton to itself and therefore is true even if the parton is in a non-singlet state with its complex conjugate (see figure 4.(b) ). therefore for a general channel the only part of equation (B1) that changes is the one dependent on the real (ladder, see figure 4.(a) ) contributions:

$$\bar{D}_A^B(x, Q^2) = \delta_A^B (1-x) d_A(k_0^2) d_B^{-1}(Q^2) + d_B^{-1}(Q^2) \sum_C \int_{zk_0^2}^{Q^2} \frac{dk^2}{k^2} \int_0^1 \frac{dz}{z} A_A^C d_B(k^2) \bar{\Phi}_C^B(z) \bar{D}_A^C\left(\frac{x}{z}, k^2\right). \quad (\text{B3})$$

Note that  $d_A$  still obeys (B2) with the singlet ( $\Phi_A^C$ ) splitting function. Trivially:

$$d_B^{-1}(Q^2) \frac{\partial}{\partial \ln(Q^2)} \left[ \bar{D}_A^B(x, Q^2) d_B(Q^2) \right] = \bar{D}_A^B(x, Q^2) d_B^{-1}(Q^2) \frac{\partial d_B(Q^2)}{\partial \ln(Q^2)} + \frac{\partial \bar{D}_A^B(x, Q^2)}{\partial \ln(Q^2)}. \quad (\text{B4})$$

Using equation (B2) and (B3) we can write:

$$\sum_C \int_0^1 \frac{dz}{z} \frac{\alpha(Q^2)}{4\pi} \bar{\Phi}_C^B(z) \bar{D}_A^C\left(\frac{x}{z}, Q^2\right) = \bar{D}_A^B(x, Q^2) \sum_C \int_0^1 z \frac{\alpha(Q^2)}{4\pi} \Phi_C^B(z) dz + \frac{\partial \bar{D}_A^B(x, Q^2)}{\partial \ln(Q^2)}, \quad (\text{B5})$$

$$\frac{\partial \bar{D}_A^B(x, Q^2)}{\partial \ln(Q^2)} = \frac{\alpha(Q^2)}{4\pi} \sum_C \int_0^1 \frac{dz}{z} \left[ \bar{\Phi}_C^B(z) \bar{D}_A^C\left(\frac{x}{z}, Q^2\right) - z^2 \Phi_B^C(z) \bar{D}_A^B(x, Q^2) \right]. \quad (\text{B6})$$

Using (6) eq. (B6) can be written as:

$$\frac{\partial D_A^B(x, Q^2)}{\partial \ln(Q^2)} = K_1 + K_2, \quad (\text{B7a})$$

$$K_1 = \frac{\alpha(Q^2)}{4\pi} \sum_C \int_0^1 \frac{dz}{z} \bar{\Phi}_C^B(z) \bar{D}_A^C\left(\frac{x}{z}, Q^2\right) - z^2 \bar{\Phi}_B^C(z) \bar{D}_A^B(x, Q^2), \quad (\text{B7b})$$

$$K_2 = \bar{D}_A^B(x, Q^2) \frac{\alpha(Q^2)}{4\pi} \sum_C \int_0^1 dz V_B^C(z) z \left[ C_B^C - \bar{C}_B^C \right]. \quad (\text{B7c})$$

The first part is finite as  $z \rightarrow 1$  and is just the regular DGLAP equation with the new kernels (which are given in table II). The second part diverges as  $z \rightarrow 1$  and therefore we need to regularize it. We'll keep the regularization given in[21]:

- Integration of  $z$  up to  $1 - \frac{\lambda^2}{k_0^2}$ , for  $\lambda$  an IR cutoff regulator
- Adding a non zero  $\Delta$  in  $V_C^B(z) \rightarrow V_C^B(z, \Delta)$  for  $\Delta = \frac{zk_0^2}{\sigma_{k_0}}$  (where  $\sigma_{k_0} = \frac{(2k_0c)^2}{c^2} \approx Q^2$ , for  $c$  the gauge fixing vector)

Define the Sudakov suppression factor:

$$\bar{S}_A(k_0^2, Q^2) = e^{-\sum_C (C_A^C - \bar{C}_A^C) \int_{k_0^2}^{Q^2} \frac{dk^2}{k^2} \frac{\alpha(k^2)}{4\pi} \int_0^{1 - \frac{\lambda^2}{k_0^2}} dz z V_A^C\left(z, \frac{zk_0^2}{\sigma_{k_0}}\right)} \quad (\text{B8})$$

Which is a properly regularized version of the version appearing in the text. Then for  $\bar{D}_A^B(x, k_0^2, Q^2) = \bar{S}_A(k_0^2, Q^2) \tilde{D}_A^B(x, k_0^2)$  eq. (B6) is reduced to (10).

**Appendix C:  $\tilde{D}_A^B$  at the Limit  $x \rightarrow 1$**

In this section, we write a derivation of (16) as the derivation in [21] is only partial, hard to generalize for different color factors, and does not include  $\tilde{D}_G^G$ . For reference we write the standard solutions of (10) in Mellin space:

$$\tilde{D}_F^F(j, \xi) = \tilde{D}^{sea}(j, \xi) + \tilde{D}^{val}(j, \xi) \quad (C1a)$$

$$\tilde{D}^{val}(j, \xi) = e^{\bar{\nu}_0 \xi} \quad (C1b)$$

$$\tilde{D}^{sea}(j, \xi) = \frac{1}{2n_f} \left[ \frac{\bar{\nu}_0 - \bar{\nu}_-}{\bar{\nu}_+ - \bar{\nu}_-} e^{\bar{\nu}_+ \xi} + \frac{\bar{\nu}_+ - \bar{\nu}_0}{\bar{\nu}_+ - \bar{\nu}_-} e^{\bar{\nu}_- \xi} - e^{\bar{\nu}_0 \xi} \right] \quad (C1c)$$

$$\tilde{D}_G^G(j, \xi) = \frac{\bar{\nu}_0 - \bar{\nu}_-}{\bar{\nu}_+ - \bar{\nu}_-} e^{\bar{\nu}_- \xi} + \frac{\bar{\nu}_+ - \bar{\nu}_0}{\bar{\nu}_+ - \bar{\nu}_-} e^{\bar{\nu}_+ \xi} \quad (C1d)$$

$$\tilde{D}_F^G(j, \xi) = \frac{\bar{\Phi}_F^G(j)}{\bar{\nu}_+ - \bar{\nu}_-} \left[ e^{\bar{\nu}_+ \xi} - e^{\bar{\nu}_- \xi} \right] \quad (C1e)$$

$$\tilde{D}_G^F(j, \xi) = \frac{\bar{\Phi}_G^F(j)}{\bar{\nu}_+ - \bar{\nu}_-} \left[ e^{\bar{\nu}_+ \xi} - e^{\bar{\nu}_- \xi} \right] \quad (C1f)$$

Where  $\xi = \frac{3}{\beta_0} \ln \left[ \frac{\alpha(k_0^2)}{\alpha(Q^2)} \right]$  and:

$$\bar{\nu}_0 = \bar{\nu}_F = \frac{1}{3} \left( - \left( \frac{6}{j} + \frac{6}{j+1} + 12(\psi(j) + \gamma_E) - 17 \right) \bar{C}_F^F - 8\bar{C}_F^G \right) \quad (C2a)$$

$$\bar{\nu}_G = -\bar{C}_G^G \left( -\frac{8(j^2 + j + 1)}{j(j^2 - 1)(j + 2)} + 4\psi(j + 1) - \frac{11}{3} + 4\gamma_E \right) - \frac{4}{3} n_f \bar{C}_G^F \quad (C2b)$$

$$\bar{\Phi}_F^G(j) = 2\bar{C}_F^G \frac{j^2 + j + 1}{j(j^2 - 1)} \quad (C2c)$$

$$\bar{\Phi}_G^F(j) = \bar{C}_G^F \frac{j^2 + j + 2}{j(j + 1)(j + 2)} \quad (C2d)$$

$$\bar{\nu}_\pm = \frac{1}{2} \left\{ \bar{\nu}_F + \bar{\nu}_G \pm \sqrt{(\bar{\nu}_F - \bar{\nu}_G)^2 + 8n_f \bar{\Phi}_F^G(j) \bar{\Phi}_G^F(j)} \right\} \quad (C2e)$$

Transforming back from Mellin to  $x$ -space is by numerically evaluating the inverse Mellin transform:

$$\tilde{D}_A^B(x, \xi) = \int \frac{dj}{2\pi i} x^{-j} \tilde{D}_A^B(j, \xi). \quad (C3)$$

For the region  $x \sim 1$  this integral can be analytically evaluated. We'll start with  $\tilde{D}^{val}$ , let's write (C3) explicitly in this case:

$$\begin{aligned}
\tilde{D}^{val}(x, \xi) &= \int \frac{dj}{2\pi i} x^{-j} e^{\bar{\nu}_0 \xi} \\
&= \int \frac{dj}{2\pi i} e^{\frac{1}{3} \left( -\left(\frac{6}{j} + \frac{6}{j+1} + 12(\psi(j) + \gamma_E) - 17\right) \bar{C}_F^F - 8\bar{C}_F^G \right) \xi - j \ln(x)}.
\end{aligned} \tag{C4}$$

This integral gets the highest contribution from its saddle point, we want to prove that this saddle point is at  $j \gg 1$ . In order to do that we'll find the maximum of the argument (aside from the singularity at  $j = 0$ ). We'll assume that this maximum is achieved at very large  $j$  and then we will see that there is indeed a maximum at this region, which will justify the assumption. At this region  $\frac{6}{j} + \frac{6}{j+1}$  are negligible and we can write  $\psi(j) \approx \ln(j) - \frac{1}{2j} \approx \ln(j)$ , therefore:

$$\begin{aligned}
0 &= \frac{d}{dj} \left[ \frac{1}{3} \left( -\left(12(\ln(j) + \gamma_E) - 17\right) \bar{C}_F^F - 8\bar{C}_F^G \right) \xi - j \ln(x) \right]_{j=j_0} \\
&= -4\xi \bar{C}_F^F \frac{1}{j_0} - \ln(x).
\end{aligned} \tag{C5}$$

So the maximum is at:

$$j_0 = -\bar{C}_F^F \frac{4\xi}{\ln(x)} \approx \bar{C}_F^F \frac{4\xi}{1-x}. \tag{C6}$$

Since  $x \sim 1$ ,  $j_0$  is very large, and so our assumption that the maximum is at very large  $j$  is justified, but only for  $\bar{C}_F^F > 0$  (we'll return to this point later on). If we now assume the major contribution to this integral comes from the proximity of this saddle point we can write it as:

$$\tilde{D}^{val}(x, \xi) \approx e^{-\xi \left[ -\left(\frac{17}{3} - 4\gamma_E\right) \bar{C}_F^F + \frac{8}{3} \bar{C}_F^G \right]} \frac{1}{2\pi i} \int e^{-4\xi \bar{C}_F^F \ln(j) - j \ln(x)} dj. \tag{C7}$$

Changing  $t = j \ln(x)$  we get:

$$\tilde{D}^{val}(x, \xi) \approx -\frac{1}{2\pi i} \frac{e^{-\xi \left[ -\left(\frac{17}{3} - 4\gamma_E\right) \bar{C}_F^F + \frac{8}{3} \bar{C}_F^G \right]}}{\ln\left(\frac{1}{x}\right)^{-4\xi \frac{N^2-1}{2N} + 1}} \int (-t)^{-4\xi \bar{C}_F^F} e^{-t} dt. \tag{C8}$$

Using the integral representation of the gamma function  $\frac{-2\pi i}{\Gamma(z)} = \int (-t)^{-z} e^{-t} dt$  and  $\ln(x) \approx x-1$  we write:

$$\tilde{D}^{val}(x, \xi) \stackrel{x \sim 1}{\approx} \frac{e^{-\xi \left[ (4\gamma_E - \frac{17}{3}) \bar{C}_F^F + \frac{8}{3} \bar{C}_F^G \right]}}{(1-x)^{1-4\xi \bar{C}_F^F} \Gamma\left(4\xi \bar{C}_F^F\right)}. \tag{C9}$$

We can now try to evaluate the other structure functions, in order to do that we'll evaluate first their components at the region of  $j_0$ .  $j_0$  is very large so we'll only keep leading terms in the expressions for  $\Phi_F^G$  and  $\Phi_G^F$ :

$$\Phi_F^G(j_0) = 2\bar{C}_F^G \frac{1}{j_0}, \quad (\text{C10a})$$

$$\Phi_G^F(j_0) = 2\bar{C}_G^F \frac{1}{j_0}. \quad (\text{C10b})$$

Both are very small and therefore we can approximate using  $\sqrt{1+\epsilon} \approx 1 + \frac{1}{2}\epsilon$  :

$$\begin{aligned} \sqrt{[\bar{\nu}_F - \bar{\nu}_G]^2 + 8n_f \Phi_F^G \Phi_G^F} &= (\bar{\nu}_F - \bar{\nu}_G) \sqrt{1 + 8n_f \frac{\left(\frac{2\bar{C}_F^G}{j_0}\right) \left(\frac{2\bar{C}_G^F}{j_0}\right)}{(\bar{\nu}_F - \bar{\nu}_G)^2}} \\ &\approx (\bar{\nu}_F - \bar{\nu}_G) \left[ 1 + \frac{1}{2} 8n_f \frac{\left(\frac{2\bar{C}_F^G}{j_0}\right) \left(\frac{2\bar{C}_G^F}{j_0}\right)}{(\bar{\nu}_F - \bar{\nu}_G)^2} \right] = (\bar{\nu}_F - \bar{\nu}_G) + 16n_f \frac{\bar{C}_F^G \bar{C}_G^F}{(\bar{\nu}_F - \bar{\nu}_G) j_0^2}. \end{aligned} \quad (\text{C11})$$

Which gives:

$$\bar{\nu}_+ \approx \bar{\nu}_F + 8n_f \bar{C}_F^G \bar{C}_G^F \frac{1}{(\bar{\nu}_F - \bar{\nu}_G) j_0^2}, \quad (\text{C12a})$$

$$\bar{\nu}_- \approx \bar{\nu}_G - 8n_f \bar{C}_F^G \bar{C}_G^F \frac{1}{(\bar{\nu}_F - \bar{\nu}_G) j_0^2}. \quad (\text{C12b})$$

Define:

$$\Delta_0 = \bar{\nu}_F(j_0) - \bar{\nu}_G(j_0). \quad (\text{C13})$$

Using the approximation:

$$\int dj f(j) e^{Mg(j)} \approx f(j_0) \int dj e^{Mg(j)} \quad (\text{C14})$$

for the saddle point  $j_0$  we can write:



$$\frac{1}{2\pi i} \int x^{-j} e^{\xi \bar{\nu}_G} = \frac{1}{2\pi i} \int x^{-j} e^{\xi(\bar{\nu}_G - \bar{\nu}_F)} e^{\xi \bar{\nu}_F} \approx e^{-\xi \Delta_0} D^{val}(x, \xi), \quad (\text{C15a})$$

$$\frac{1}{2\pi i} \int x^{-j} e^{\xi \bar{\nu}_-} \approx e^{-\xi \Delta_0 - \xi 8n_f \bar{C}_F^G \bar{C}_G^F \frac{1}{\Delta_0 j_0^2}} D^{val}(x, \xi), \quad (\text{C15b})$$

$$\frac{1}{2\pi i} \int x^{-j} e^{\xi \bar{\nu}_+} \approx e^{\xi 8n_f \bar{C}_F^G \bar{C}_G^F \frac{1}{\Delta_0 j_0^2}} D^{val}(x, \xi). \quad (\text{C15c})$$

We can also write, at the saddle point  $j_0$ :

$$\frac{\bar{\nu}_+ - \bar{\nu}_0}{\bar{\nu}_+ - \bar{\nu}_-} \approx \frac{1}{\Delta_0 + \frac{1}{\Delta_0} \frac{16n_f \bar{C}_F^G \bar{C}_G^F}{j_0^2}} \frac{1}{\Delta_0} 4n_f \frac{N^2 - 1}{2N} \frac{1}{j_0^2} = \frac{\frac{1}{\Delta_0} \frac{8n_f \bar{C}_F^G \bar{C}_G^F}{j_0^2} \left( \Delta_0 - \frac{1}{\Delta_0} \frac{16n_f \bar{C}_F^G \bar{C}_G^F}{j_0^2} \right)}{(\Delta_0)^2 - \left( \frac{1}{\Delta_0} \frac{16n_f \bar{C}_F^G \bar{C}_G^F}{j_0^2} \right)^2}, \quad (\text{C16a})$$

$$\frac{\bar{\nu}_0 - \bar{\nu}_-}{\bar{\nu}_+ - \bar{\nu}_-} \approx \frac{\Delta_0 + \frac{1}{\Delta_0} \frac{8n_f \bar{C}_F^G \bar{C}_G^F}{j_0^2}}{\Delta_0 + \frac{1}{\Delta_0} \frac{16n_f \bar{C}_F^G \bar{C}_G^F}{j_0^2}} = \frac{\left( \Delta_0 + \frac{1}{\Delta_0} \frac{8n_f \bar{C}_F^G \bar{C}_G^F}{j_0^2} \right) \left( \Delta_0 - \frac{1}{\Delta_0} \frac{16n_f \bar{C}_F^G \bar{C}_G^F}{j_0^2} \right)}{(\Delta_0)^2 - \left( \frac{1}{\Delta_0} \frac{16n_f \bar{C}_F^G \bar{C}_G^F}{j_0^2} \right)^2}. \quad (\text{C16b})$$

Neglecting terms of order  $\frac{1}{j_0^4}$  in both numerator and denominator we arrive at:

$$\frac{\bar{\nu}_+ - \bar{\nu}_0}{\bar{\nu}_+ - \bar{\nu}_-} \approx \frac{8n_f \bar{C}_F^G \bar{C}_G^F}{j_0^2 \Delta_0^2}, \quad (\text{C17a})$$

$$\frac{\bar{\nu}_0 - \bar{\nu}_-}{\bar{\nu}_+ - \bar{\nu}_-} \approx \frac{\Delta_0^2 - \frac{8n_f \bar{C}_F^G \bar{C}_G^F}{j_0^2}}{\Delta_0^2} = 1 - 8n_f \bar{C}_F^G \bar{C}_G^F \frac{1}{\Delta_0^2 j_0^2}. \quad (\text{C17b})$$

Using All these together let us write:

$$\tilde{D}_F^G(x, \xi) \approx \frac{\Phi_F^G(j_0)}{\bar{\nu}_+ - \bar{\nu}_-} \left[ e^{\frac{\xi 8n_f \bar{C}_F^G \bar{C}_G^F}{\Delta_0 j_0^2}} \tilde{D}^{val}(x, \xi) - e^{-\xi \Delta_0 - \frac{\xi 8n_f \bar{C}_F^G \bar{C}_G^F}{\Delta_0 j_0^2}} \tilde{D}^{val}(x, \xi) \right]. \quad (\text{C18})$$

Keeping terms only up to  $\frac{1}{j_0}$  we have:

$$\tilde{D}_F^G(x, \xi) \approx \frac{2\bar{C}_F^G}{\Delta_0 j_0} \left[ 1 - e^{-\xi \Delta_0} \right] D^{val}(x, \xi). \quad (\text{C19})$$

For  $\tilde{D}^{sea}(x, \xi)$  we'll have to keep terms up to  $\frac{1}{j_0^2}$  and to keep the equations short write  $\bar{Z}_0 = \frac{8n_f \bar{C}_F^G \bar{C}_G^F}{\Delta_0^2}$ .

$$\begin{aligned}
D^{sea}(x, \xi) &\approx \frac{1}{2n_f} \left[ \left( 1 - \frac{\bar{Z}_0}{j_0^2} \right) e^{\frac{\xi \Delta_0 \bar{Z}_0}{j_0^2}} + \frac{\bar{Z}_0}{j_0^2} e^{-\xi \Delta_0 - \frac{\xi \Delta_0 \bar{Z}_0}{j_0^2}} - 1 \right] \tilde{D}^{val}(x, \xi) \\
&\approx \frac{1}{2n_f} \left[ e^{\xi 8n_f \bar{C}_F \bar{C}_G \frac{1}{\Delta_0 j_0^2}} - 1 + \frac{\bar{Z}_0}{j_0^2} \left( -e^{\frac{\xi \Delta_0 \bar{Z}_0}{j_0^2}} + e^{-\xi \Delta_0 - \frac{\xi \Delta_0 \bar{Z}_0}{j_0^2}} \right) \right] \tilde{D}^{val}(x, \xi) \\
&\approx \frac{1}{2n_f} \left[ \left( e^{\frac{\xi \Delta_0 \bar{Z}_0}{j_0^2}} - 1 \right) + \frac{\bar{Z}_0}{j_0^2} \left( -e^{\frac{\xi \Delta_0 \bar{Z}_0}{j_0^2}} + e^{-\xi \Delta_0} \left( e^{-\frac{\xi \Delta_0 \bar{Z}_0}{j_0^2}} \right) \right) \right] \tilde{D}^{val}(x, \xi) \\
&\approx \frac{1}{2n_f} \left[ \frac{\xi \Delta_0 \bar{Z}_0}{j_0^2} + \frac{\bar{Z}_0}{j_0^2} \left( -1 - \frac{\xi \Delta_0 \bar{Z}_0}{j_0^2} + e^{-\xi \Delta_0} \left( 1 - \frac{\xi \Delta_0 \bar{Z}_0}{j_0^2} \right) \right) \right] \tilde{D}^{val}(x, \xi) \\
&\approx 4 \frac{\bar{C}_F \bar{C}_G}{\Delta_0^2 j_0^2} \left[ \Delta_0 \xi - 1 + e^{-\xi \Delta_0} + \frac{\xi \Delta_0 \bar{Z}_0}{j_0^2} \left( 1 - e^{-\xi \Delta_0} \right) \right] \tilde{D}^{val}(x, \xi). \tag{C20}
\end{aligned}$$

Neglecting again any  $\frac{1}{j_0^4}$  terms we arrive at:

$$\tilde{D}^{sea}(x, \xi) \approx 4 \frac{\bar{C}_F \bar{C}_G}{\Delta_0^2 j_0^2} \left[ \Delta_0 \xi - 1 + e^{-\xi \Delta_0} \right] \tilde{D}^{val}(x, \xi). \tag{C21}$$

To compute  $\tilde{D}_G^G$  and  $\tilde{D}_F^G$  we would want to take the saddle point at the value suitable to  $\bar{\nu}_G$  instead of  $\bar{\nu}_F$ . The change is very easy and we have:

$$j_G = \bar{C}_G \frac{4\xi}{1-x}, \tag{C22}$$

$$\frac{1}{2\pi i} \int dx x^{-j} e^{\xi \bar{\nu}_G} \approx e^{\xi \left[ \bar{C}_G \left( \frac{11}{3} - 4\gamma_E \right) - \frac{4}{3} n_f \bar{C}_G^F \right]} \frac{(1-x)^{4\xi \bar{C}_G^G - 1}}{\Gamma(4\xi \bar{C}_G^G)} := G(x, \xi). \tag{C23}$$

By the same reasoning we now approximate:

$$\frac{1}{2\pi i} \int dx x^{-j} e^{\xi \bar{\nu}_F} \approx e^{\Delta_0 \xi} G(x, \xi), \tag{C24a}$$

$$\bar{\nu}_+ \approx \bar{\nu}_F + \frac{8n_f \bar{C}_F \bar{C}_G^F}{\Delta_0 j_G^2}, \tag{C24b}$$

$$\bar{\nu}_- \approx \bar{\nu}_G - \frac{8n_f \bar{C}_F \bar{C}_G^F}{\Delta_0 j_G^2}. \tag{C24c}$$

And so on. We can therefore compute:

$$\begin{aligned}
\tilde{D}_G^G(x, \xi) &\approx \frac{8n_f \bar{C}_F^G \bar{C}_G^F}{\Delta_0^2 j_0^2} e^{\Delta_0 \xi + \frac{\xi 8n_f \bar{C}_F^G \bar{C}_G^F}{\Delta_0 j_G^2}} G(x, \xi) + \left(1 - \frac{8n_f \bar{C}_F^G \bar{C}_G^F}{\Delta_0^2 j_0^2}\right) e^{-\frac{\xi 8n_f \bar{C}_F^G \bar{C}_G^F}{\Delta_0 j_G^2}} G(x, \xi) \\
&\approx \left[ \frac{8n_f \bar{C}_F^G \bar{C}_G^F}{\Delta_0^2 j_0^2} \left(1 + \Delta_0 \xi + \frac{\xi 8n_f \bar{C}_F^G \bar{C}_G^F}{\Delta_0 j_G^2}\right) + \left(1 - \frac{8n_f \bar{C}_F^G \bar{C}_G^F}{\Delta_0^2 j_0^2}\right) \left(1 - \frac{\xi 8n_f \bar{C}_F^G \bar{C}_G^F}{\Delta_0 j_G^2}\right) \right] G(x, \xi).
\end{aligned} \tag{C25}$$

The leading term in this solution is clearly:

$$\tilde{D}_G^G(x, \xi) \approx G(x, \xi). \tag{C26}$$

Which is analog to  $D^{val}$  for quark. We also have:

$$\begin{aligned}
\tilde{D}_G^F &\approx \frac{2\bar{C}_G^F}{j_G \Delta_0} \left[ e^{\Delta_0 \xi + \frac{\xi 8n_f \bar{C}_F^G \bar{C}_G^F}{\Delta_0 j_G^2}} D_G^G(x, \xi) - e^{-\frac{\xi 8n_f \bar{C}_F^G \bar{C}_G^F}{\Delta_0 j_G^2}} D_G^G(x, \xi) \right] \\
&\approx \frac{2\bar{C}_G^F}{j_G \Delta_0} \left[ e^{\Delta_0 \xi} \left(1 + \frac{\xi 8n_f \bar{C}_F^G \bar{C}_G^F}{\Delta_0 j_G^2}\right) - \left(1 - \frac{\xi 8n_f \bar{C}_F^G \bar{C}_G^F}{\Delta_0 j_G^2}\right) \right] D_G^G(x, \xi) \\
&\approx \frac{2\bar{C}_G^F}{j_G \Delta_0} \left[ e^{\Delta_0 \xi} - 1 \right] \tilde{D}_G^G(x, \xi).
\end{aligned} \tag{C27}$$

Here we neglected any  $\frac{1}{j_G^2}$  terms. To summarize:

$$\tilde{D}^{val}(x, \xi) \stackrel{x \sim 1}{\approx} \tilde{D}_F^F(x, \xi) \approx \frac{e^{-\xi \left[ (4\gamma_E - \frac{17}{3}) \bar{C}_F^F + \frac{8}{3} \bar{C}_F^G \right]}}{(1-x)^{1-4\xi \bar{C}_F^F} \Gamma(4\xi \bar{C}_F^F)}, \tag{C28a}$$

$$\tilde{D}^{sea}(x, \xi) \approx 4 \frac{\bar{C}_F^G \bar{C}_G^F}{\Delta_0^2 j_0^2} \left[ \Delta_0 \xi - 1 + e^{-\xi \Delta_0} \right] \tilde{D}^{val}(x, \xi), \tag{C28b}$$

$$\tilde{D}_F^G(x, \xi) \approx \frac{2\bar{C}_F^G}{\Delta_0 j_0} \left[ 1 - e^{-\xi \Delta_0} \right] D^{val}(x, \xi), \tag{C28c}$$

$$\tilde{D}_G^G(x, \xi) \approx e^{\xi \left[ \bar{C}_G^G \left( \frac{11}{3} - 4\gamma_E \right) - \frac{4}{3} n_f \bar{C}_G^F \right]} \frac{(1-x)^{4\xi \bar{C}_G^G - 1}}{\Gamma(4\xi \bar{C}_G^G)}, \tag{C28d}$$

$$\tilde{D}_G^F \approx \frac{2\bar{C}_G^F}{j_G \Delta_0} \left[ e^{\Delta_0 \xi} - 1 \right] \tilde{D}_G^G(x, \xi). \tag{C28e}$$

At  $x \rightarrow 1$   $j_0, j_G \propto \frac{1}{1-x}$  and  $\Delta_0 \propto \ln(1-x)$  and therefore we get (C9).

### Appendix D: Regularizing Divergent Integrals

In section IID we have introduced the regularization:

$$\int_0^1 dx \frac{f(x)}{x^\lambda} := \int_0^1 \frac{f(x) - f(0)}{x^\lambda} dx + \frac{f(0)}{1-\lambda}. \quad (\text{D1})$$

It's natural to ask whether regularization is well defined, particularly if we change the range of integration. We'll prove in the 1 dimensional case that this regularization is well defined and get the same value for every range of integration that contains all the values for which  $f(x) \neq 0$ . Let  $f(x) = \theta(x - x_0) \tilde{f}(x)$  be a function that is smooth and bounded in the region  $[0, x_0)$ , we need to understand how to generalize (D1) to a general integration interval. The generalization of the first term on the r.h.s is trivial: just change the integration to the new region. The generalization of the second term is a bit less trivial, this term is defined as the analytical continuation of the integral

$$\int_0^1 dx \frac{f(0)}{x^\lambda} = \frac{f(0)}{1-\lambda} \quad (\text{D2})$$

for  $\lambda < 1$ . When we change the integration limit we then get

$$\int_0^y dx \frac{f(0)}{x^\lambda} = y^{1-\lambda} \frac{f(0)}{1-\lambda}, \quad (\text{D3})$$

so we can define for  $y > x_0$ :

$$I_y = \int_0^y dx \frac{f(x)}{x^\lambda} := \int_0^y \frac{f(x) - f(0)}{x^\lambda} dx + y^{1-\lambda} \frac{f(0)}{1-\lambda}. \quad (\text{D4})$$

Note that we changed the integration limit in the first term and the coefficient in the second term, as discussed above. Now we need to prove that  $I_y = I_{x_0}$  for  $1 < \lambda < 2$  (for  $\lambda < 1$  this statement is trivial). Write:

$$I_y = \int_0^{x_0} \frac{f(x) - f(0)}{x^\lambda} dx + \int_{x_0}^y \frac{f(x) - f(0)}{x^\lambda} dx + y^{1-\lambda} \frac{f(0)}{1-\lambda}, \quad (\text{D5})$$

using the fact that  $f(x) = 0$  for  $x_0 < x < y$  we write this equation as:

$$I_y = \int_0^{x_0} \frac{f(x) - f(0)}{x^\lambda} dx - \int_{x_0}^y \frac{f(0)}{x^\lambda} dx + y^{1-\lambda} \frac{f(0)}{1-\lambda}. \quad (\text{D6})$$

The integral in the middle term converges because  $x_0 > 0$  so we can write it as:

$$I_y = \int_0^{x_0} \frac{f(x) - f(0)}{x^\lambda} dx - y^{1-\lambda} \frac{f(0)}{1-\lambda} + x_0^{1-\lambda} \frac{f(0)}{1-\lambda} + y^{1-\lambda} \frac{f(0)}{1-\lambda} \quad (\text{D7})$$

$$= \int_0^{x_0} \frac{f(x) - f(0)}{x^\lambda} dx + x_0^{1-\lambda} \frac{f(0)}{1-\lambda} = I_{x_0}. \quad (\text{D8})$$

As was needed. This computation proves the 1 dimensional case of this regularization is well defined, note however we needed to change both terms of (D1) and not only the integration limit of the first term. In the 2 dimensional case, the proof is harder because integration regions in  $2d$  can be much more complex, we'll therefore only see an example of this phenomenon. The definition of  $F(z_1, z_2)$  in (42a) contain the hadron structure function  $G_h^{A'}\left(\frac{x_1}{z_1} + \frac{x_2}{z_2}; k^2\right)$  which satisfy  $G_h^{A'}\left(\frac{x_1}{z_1} + \frac{x_2}{z_2}; k^2\right) \equiv 0$  for  $\frac{x_1}{z_1} + \frac{x_2}{z_2} > 1$ . We could therefore take the integrals in (40) with this condition instead of over the entire region  $[x_1, 1] \times [x_2, 1]$ . This condition would mean to write the four parts of this integral as:

$$\tilde{I} = \int \int_{\frac{x_1}{z_1} + \frac{x_2}{z_2} > 1} dz_1 dz_2 \frac{F(z_1, z_2)}{(1-z_1)^{1-g_1} (1-z_2)^{1-g_2}}, \quad (\text{D9})$$

$$\tilde{I} = \tilde{I}_A + \tilde{I}_B + \tilde{I}_C + \tilde{I}_D, \quad (\text{D10a})$$

$$\tilde{I}_A = \int \int_{\frac{x_1}{z_1} + \frac{x_2}{z_2} > 1} dz_1 dz_2 \frac{F(z_1, z_2) - F(1, z_2) - F(z_1, 1) + F(1, 1)}{(1 - z_1)^{1-g_1} (1 - z_2)^{1-g_2}}, \quad (\text{D10b})$$

$$\begin{aligned} \tilde{I}_B &= \int \int_{\frac{x_1}{z_1} + \frac{x_2}{z_2} > 1} dz_1 dz_2 \frac{F(z_1, 1) - F(1, 1)}{(1 - z_1)^{1-g_1} (1 - z_2)^{1-g_2}}, \\ &= \int_{x_1}^1 dz_1 \frac{F(z_1, 1) - F(1, 1)}{(1 - z_1)^{1-g_1}} \int_{\frac{\frac{x_2}{1-z_1}}{1-\frac{x_1}{z_1}}}^1 dz_2 \frac{1}{(1 - z_2)^{1-g_2}} \\ &= \int_{x_1}^1 dz_1 \frac{F(z_1, 1) - F(1, 1)}{(1 - z_1)^{1-g_1}} C(x_1, x_2, z_1, g_2) \end{aligned} \quad (\text{D10c})$$

$$\begin{aligned} \tilde{I}_C &= \int \int_{\frac{x_1}{z_1} + \frac{x_2}{z_2} > 1} dz_1 dz_2 \frac{F(1, z_2) - F(1, 1)}{(1 - z_1)^{1-g_1} (1 - z_2)^{1-g_2}}, \\ &= \int_{x_2}^1 dz_2 \frac{F(1, z_2) - F(1, 1)}{(1 - z_2)^{1-g_2}} \int_{\frac{\frac{x_1}{1-z_2}}{1-\frac{x_2}{z_2}}}^1 dz_1 \frac{1}{(1 - z_1)^{1-g_1}} \\ &= \int_{x_2}^1 dz_2 \frac{F(1, z_2) - F(1, 1)}{(1 - z_2)^{1-g_2}} C(x_2, x_1, z_2, g_1) \end{aligned} \quad (\text{D10d})$$

$$\tilde{I}_D = \int \int_{\frac{x_1}{z_1} + \frac{x_2}{z_2} > 1} dz_1 dz_2 \frac{F(1, 1)}{(1 - z_1)^{1-g_1} (1 - z_2)^{1-g_2}} = D(x_1, x_2, g_1, g_2) F(1, 1). \quad (\text{D10e})$$

Where  $C$  and  $D$  are the analytic solutions of these integrals, which has a complex form as a combination of hypergeometric functions that can be extended to every value of  $g_1$  and  $g_2$ . Although this expression is much more complex than (40) numerical calculations show it's actually the same.

## Appendix E: Rules for Color Projectors

### 1. Exact Form of Projectors

We define the usual color projectors for two gluons into irreducible representations which commonly appear in the literature (see for example [13, 42, 43]). We use however the notations of [40, 41] both for the names of the representations  $\alpha = \{8_a, 10, 1, 8_s, 27, 0\}$  (the order is important) and for their definitions. The names are of the “ $SU(3)$ ” dimensions (even though in the paper we keep the general  $SU(N)$  representations). Also as in [40, 41] 10 is actually the (direct) sum of

the two irreducible representations  $\overline{10} + 10$ . In the following, we sum over repeated indices both representation indices (marked in Greek letters) and color (marked in small Latin characters).

$$P_{ab;cd}^1 = \frac{1}{N^2 - 1} \delta_{ab} \delta_{cd}, \quad (\text{E1a})$$

$$P_{ab;cd}^{8_a} = - \frac{f^{aeb} f^{cde}}{N}, \quad (\text{E1b})$$

$$P_{ab;cd}^{8_s} = \frac{N}{N^2 - 4} d_{abe} d_{cde}, \quad (\text{E1c})$$

$$P_{ab;cd}^{10} = \frac{1}{2} (\mathbf{1}_{ab;cd} - X_{ab;cd}) - P_{ab;cd}^{8_a}, \quad (\text{E1d})$$

$$P_{ab;cd}^{27} = \frac{1}{4} (\mathbf{1}_{ab;cd} + X_{ab;cd}) - \frac{N-2}{2N} P_{ab;cd}^{8_s} - \frac{N-1}{2N} P_{ab;cd}^1 + (W_{ab;cd}^+ + W_{ab;cd}^-), \quad (\text{E1e})$$

$$P_{ab;cd}^0 = \frac{1}{4} (\mathbf{1}_{ab;cd} + X_{ab;cd}) - \frac{N+2}{2N} P_{ab;cd}^{8_s} - \frac{N+1}{2N} P_{ab;cd}^1 + (W_{ab;cd}^+ + W_{ab;cd}^-). \quad (\text{E1f})$$

Where  $N$  is the number of colors in  $SU(N)$  and:

$$\mathbf{1}_{ab;cd} = \delta_{ac} \delta_{bd}, \quad (\text{E2a})$$

$$X_{ab;cd} = \delta_{ad} \delta_{bc}, \quad (\text{E2b})$$

$$W_{ab;cd}^- = \text{Tr} \left( t^b t^c t^a t^d \right), \quad (\text{E2c})$$

$$W_{ab;cd}^+ = \text{Tr} \left( t^b t^d t^a t^c \right). \quad (\text{E2d})$$

## 2. Properties

We list here some of the properties of these projectors we have used in the body of the text. Unless otherwise noted they are cited from [41] where we direct to the equations in that paper.

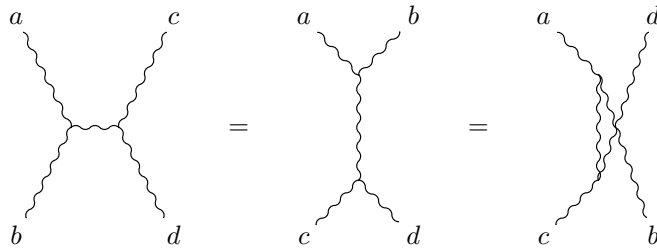
### a. Projectors

The above defined are projectors (eq. A.17), i.e:

$$P_{ab;cd}^\alpha P_{cd;ef}^\beta = \delta_{\alpha\beta} P_{ab;ef}^\alpha.$$

### b. Symmetries

Each representation is either symmetric or anti-symmetric with respect to interchanging incoming (outgoing) gluons. this property means that:

Figure 23.  $s, t, u$  channels

$$P_{ab;cd}^\alpha = r_\alpha P_{ba;cd}^\alpha = r_\alpha P_{ab;dc}^\alpha. \quad (\text{E3})$$

Here  $r_\alpha = \{-1, -1, 1, 1, 1, 1\}$  depend on the representation. Since each projector is either symmetric or anti-symmetric if we interchange both its “incoming” (first two) or “outgoing” (last two) indices it’ll remain the same (anti-symmetric projectors acquire a  $(-1)^2 = 1$  factor):

$$P_{ab;cd}^\alpha = P_{ba;dc}^\alpha. \quad (\text{E4})$$

Also, all of the projectors are symmetric in incoming and outgoing indices (proof in section E 3):

$$P_{ab;cd}^\alpha = P_{cd;ab}^\alpha. \quad (\text{E5})$$

### c. Change in Basis

We could also work in  $t$  or  $u$ -channel projectors which are simply:

$$P_{ab;cd} = P_{ac;bd}^{(t)} = P_{ac;db}^{(u)}, \quad (\text{E6})$$

graphically seen in figure 23. We can use the so called “re-projection” matrix (eq 2.31) to find that:

$$P_{ab;cd}^\alpha = [K_{ts}]^{\alpha\beta} P_{ac;bd}^\beta, \quad (\text{E7})$$



$$P_{ab;cd}^\alpha = [K_{su}]^{\alpha\beta} P_{ad;bc}^\beta, \quad (\text{E8})$$

$$P_{ab;cd}^\alpha = [K_{us}]^{\alpha\beta} P_{ac;db}^\beta. \quad (\text{E9})$$

From these equations we can see that  $K_{ts} = K_{st} = K_{ts}^{-1}$  and that  $K_{su}^2 = K_{us} = K_{su}^{-1}$ . The explicit form of  $K_{ts}$ ,  $K_{su}$  and  $K_{us}$  is given in [41] eq A.28 and the paragraph thereafter:

$$K_{ts} = \begin{pmatrix} \frac{1}{2} & 0 & 1 & \frac{1}{2} & -\frac{1}{N} & \frac{1}{N} \\ 0 & \frac{1}{2} & \frac{1}{2}(N^2 - 4) & -1 & \frac{2-N}{2N} & \frac{-N-2}{2N} \\ \frac{1}{N^2-1} & \frac{1}{N^2-1} & \frac{1}{N^2-1} & \frac{1}{N^2-1} & \frac{1}{N^2-1} & \frac{1}{N^2-1} \\ \frac{1}{2} & -\frac{2}{N^2-4} & 1 & \frac{N^2-12}{2N^2-8} & \frac{1}{N+2} & -\frac{1}{N-2} \\ -\frac{N(N+3)}{4(N+1)} & -\frac{N(N+3)}{4(N+1)(N+2)} & \frac{N^2(N+3)}{4(N+1)} & \frac{N^2(N+3)}{4(N+1)(N+2)} & \frac{N^2+N+2}{4(N+1)(N+2)} & \frac{N+3}{4(N+1)} \\ \frac{(N-3)N}{4(N-1)} & -\frac{(N-3)N}{4(N-2)(N-1)} & \frac{(N-3)N^2}{4(N-1)} & -\frac{(N-3)N^2}{4(N-2)(N-1)} & \frac{N-3}{4(N-1)} & \frac{N^2-N+2}{4(N-2)(N-1)} \end{pmatrix}, \quad (\text{E10})$$

$$K_{su} = \begin{pmatrix} -\frac{1}{2} & 0 & -1 & -\frac{1}{2} & \frac{1}{N} & -\frac{1}{N} \\ 0 & -\frac{1}{2} & \frac{1}{2}(4 - N^2) & 1 & \frac{N-2}{2N} & \frac{N+2}{2N} \\ \frac{1}{N^2-1} & \frac{1}{N^2-1} & \frac{1}{N^2-1} & \frac{1}{N^2-1} & \frac{1}{N^2-1} & \frac{1}{N^2-1} \\ \frac{1}{2} & -\frac{2}{N^2-4} & 1 & \frac{N^2-12}{2N^2-8} & \frac{1}{N+2} & -\frac{1}{N-2} \\ -\frac{N(N+3)}{4(N+1)} & -\frac{N(N+3)}{4(N+1)(N+2)} & \frac{N^2(N+3)}{4(N+1)} & \frac{N^2(N+3)}{4(N+1)(N+2)} & \frac{N^2+N+2}{4(N+1)(N+2)} & \frac{N+3}{4(N+1)} \\ \frac{(N-3)N}{4(N-1)} & -\frac{(N-3)N}{4(N-2)(N-1)} & \frac{(N-3)N^2}{4(N-1)} & -\frac{(N-3)N^2}{4(N-2)(N-1)} & \frac{N-3}{4(N-1)} & \frac{N^2-N+2}{4(N-2)(N-1)} \end{pmatrix}, \quad (\text{E11})$$

$$K_{us} = \begin{pmatrix} -\frac{1}{2} & 0 & 1 & \frac{1}{2} & -\frac{1}{N} & \frac{1}{N} \\ 0 & -\frac{1}{2} & \frac{1}{2}(N^2 - 4) & -1 & \frac{2-N}{2N} & \frac{-N-2}{2N} \\ -\frac{1}{N^2-1} & -\frac{1}{N^2-1} & \frac{1}{N^2-1} & \frac{1}{N^2-1} & \frac{1}{N^2-1} & \frac{1}{N^2-1} \\ -\frac{1}{2} & \frac{2}{N^2-4} & 1 & \frac{N^2-12}{2N^2-8} & \frac{1}{N+2} & -\frac{1}{N-2} \\ \frac{N(N+3)}{4(N+1)} & \frac{N(N+3)}{4(N+1)(N+2)} & \frac{N^2(N+3)}{4(N+1)} & \frac{N^2(N+3)}{4(N+1)(N+2)} & \frac{N^2+N+2}{4(N+1)(N+2)} & \frac{N+3}{4(N+1)} \\ -\frac{(N-3)N}{4(N-1)} & \frac{(N-3)N}{4(N-2)(N-1)} & \frac{(N-3)N^2}{4(N-1)} & -\frac{(N-3)N^2}{4(N-2)(N-1)} & \frac{N-3}{4(N-1)} & \frac{N^2-N+2}{4(N-2)(N-1)} \end{pmatrix}. \quad (\text{E12})$$

Which indeed obey the rules above.

$$\begin{aligned}
 V_{ab;cd} = & \quad \begin{array}{c} a \quad c \\ \diagdown \quad / \\ \text{---} \\ \diagup \quad \diagdown \\ b \quad d \end{array} \quad = N P_{ac;bd}^{(t)\delta_s} = N [K_{ts}]^{\delta_s \alpha} P_{ab,cd}^\alpha
 \end{aligned}$$

Figure 24. Interaction force

*d. Interaction Force*

Suppose we connect the two incoming gluons with another gluon. This gluon has the form shown in figure 24, therefore:

$$\begin{aligned}
 f^{aea'} f^{beb'} P_{ab;cd}^\alpha &= V_{a'b';ab} P_{ab;cd}^\alpha \\
 &= N [K_{ts}]^{\delta_s \alpha} P_{a'b';ab}^\alpha P_{ab;cd}^\alpha \\
 &= N [K_{ts}]^{\delta_s \alpha} P_{a'b';cd}^\alpha \\
 &= c_\alpha P_{a'b';cd}^\alpha,
 \end{aligned} \tag{E13}$$

for  $c_\alpha = \left\{ \frac{N}{2}, 0, N, \frac{N}{2}, -1, 1 \right\}$ .

*e. Dimensions of the Representation*

By contracting two indices of the projector:

$$P_{ab;ab}^\alpha = K^\alpha. \tag{E14}$$

Here (eq. 3.3):

$$K_\alpha = \left\{ N^2 - 1, \frac{1}{2} (N^2 - 4) (N^2 - 1), 1, N^2 - 1, \frac{1}{4} (N - 1) N^2 (N + 3), \frac{1}{4} (N - 3) N^2 (N + 1) \right\}$$

is the dimension of the representation. This relation has the consequence:

$$P_{ab;cb}^\alpha = \delta_{ac} \frac{K^\alpha}{N^2 - 1}. \tag{E15}$$

*f. Completeness Relation*

We have that (eq. 3.5):

$$\mathbf{1} = \delta_{ac}\delta_{bd} = \sum_{\alpha} P_{ab;cd}^{\alpha}. \quad (\text{E16})$$

### 3. Proof of Incoming-Outgoing Symmetry

We haven't found proof of this relation in the literature. Although the proof is easy we'll write it here. We'll prove this relation for every representation individually using the explicit forms in (E1):

1 It's trivial  $\frac{1}{N^2-1}\delta_{ab}\delta_{cd} = \frac{1}{N^2-1}\delta_{cd}\delta_{ab}$ .

8<sub>s</sub> It's trivial  $\frac{N}{N^2-4}d_{abe}d_{cde} = \frac{N}{N^2-4}d_{cde}d_{abe}$ .

8<sub>a</sub> It's somewhat less trivial but still easy to see that  $-\frac{f^{acb}f^{cde}}{N} = -\frac{f^{ceb}f^{fabe}}{N}$ . Note that we change the order in both form factors so the total sign is kept  $(-1)^2 = 1$ .

10 We note that  $\mathbf{1}$  and  $X$  have this symmetry. Then using the explicit form the symmetry is easy to see since it's true to each part. It should be noted that this symmetry is not true for either  $\overline{10}, 10$  alone, but is true for the sum  $\overline{10} + 10$ .

27/0 This symmetry gives:

$$W_+ = Tr \left( t^b t^d t^a t^c \right) \rightarrow Tr \left( t^b t^c t^a t^d \right) = W_- \quad (\text{E17})$$

and therefore  $W_+ + W_-$  is symmetric. We see that both  $P^0$  and  $P^{27}$  are symmetric using their explicit forms (as they can be written as a combination of  $P^1, P^{8_s}, \mathbf{1}, X$ , and  $W_+ + W_-$ ).

## Appendix F: Comments on Different Formalisms

In this Appendix we shall make comments on the relation of the formalism used in this paper for the calculation of  ${}_2GPD$ , and the formalism used in [8, 11]

### 1. The Sudakov Suppression Factor.

First, consider the calculation of Sudakov formfactor using DDT procedure. The anomalous dimensions in equation (5), that include LO and NLO transverse logarithms, exactly coincide with

the logarithms corresponding to the anomalous dimensions  $\gamma_\mu$  in [8, 11] (see e.g. Eq. (11) in [11] for octet channel and extension to other channels in [8, 15]). By LO we mean the double logarithmic term first found in [13], and NLO means single transverse logarithms.

Let us consider the issue of next to leading transverse logarithms in Sudakov formfactor in more detail. We shall see that the full answer coming from DGLAP equations is universal, both for leading (LO) and next to leading (NLO) logarithms. Also the double logarithmic (LO) piece in Sudakov formfactor is universal. On the other hand, the distribution between single logarithms in DGLAP like equation and Sudakov formfactor may depend on regularisation scheme.

Recall that the full evolution equation has the form (5) and its solution in general can be written in the factorized form (8):

$$\bar{D}_A^B(x, k^2, Q^2) = S_A^B(k^2, Q^2) \cdot \tilde{D}_A^B(x, k^2, Q^2) \quad (\text{F1})$$

The Sudakov formfactor contains, for general channel double and single transverse logs, but no dependence on longitudinal variable  $x$ , while the function  $\tilde{D}_A^B(x, k^2, Q^2)$  contains only single logarithms and satisfies DGLAP like integrodifferential equation. In this paper we used the DDT regularisation scheme with the  $z = 1$  singularity regularised by

$$\frac{1}{1 - z + \Delta}, \quad \Delta = k^2/Q^2, \quad (\text{F2})$$

while it is conventional to use Altarelli-Parisi kernels where the regularisation in the  $z = 1$  limit is given by  $+$  prescription and delta functions, i.e.

$$P_{qq}(z) = \frac{2z}{(1-z)_+} + 1 - z - \frac{3}{2}\delta(1-z) \quad (\text{F3})$$

Here we shall call this scheme AP scheme to distinguish from DDT regularisation. We shall show that both schemes lead to the same full evolution equation for full function  $\bar{D}$ , but the natural split between Sudakov formfactor  $S$  and function  $\tilde{D}$  depends on the scheme, although the product of course remains the same.

To illustrate this point we shall consider here the equation for fermion ladder  $D_F^F$ . There are two possibilities: the singlet and the octet channel. Consider first the singlet channel.

#### *a. Proof of the Singlet Case*

First we'll prove the equivalence of DGLAP evolution equations in the singlet case, between "DDT formalism" which we used in the text and the perhaps more common Altarelli-Parisi formalism. The evolution equation in [11] is:

$$\frac{\partial D_F^F(x, k^2, Q^2)}{\partial \ln(Q)} = \frac{\alpha_s}{\pi} \int_x^1 \frac{dz}{z} C_F^F P_{qq}(z) D_F^F\left(\frac{x}{z}, Q^2\right) \quad (\text{F4})$$

where  $P_{qq}$  is the corresponding AP kernel, so that the equation has the form:

$$\begin{aligned} \frac{\partial D_F^F(x)}{\partial \ln(Q^2)} &= \frac{\alpha_s}{2\pi} \int_x^1 \frac{dz}{z} C_F^F \left[ \frac{1+z^2}{(1-z)_+} + \frac{3}{2} \delta(1-z) \right] D_F^F\left(\frac{x}{z}\right) = \\ &= \frac{\alpha_s}{2\pi} \int_0^1 \frac{dz}{z} \left\{ C_F^F \left[ \frac{1+z^2}{1-z} \right] D_F^F\left(\frac{x}{z}\right) - z C_F^F \left( \frac{2}{1-z} - \frac{3}{2} \right) D_F^F(x) \right\} \end{aligned} \quad (\text{F5})$$

where we explicitly carried the + subtraction. On the other hand the corresponding equation in DDT scheme [21], reads:

$$\begin{aligned} \frac{\partial D_F^F(x)}{\partial \ln(Q^2)} &= \frac{\alpha_s}{4\pi} \int_0^1 \frac{dz}{z} \left\{ \Phi_F^F(z) D_F^F\left(\frac{x}{z}\right) - z^2 D_F^F(x) (\Phi_F^F(z) + \Phi_F^G(z)) \right\} = \\ &= \frac{\alpha_s}{4\pi} \int_0^1 \frac{dz}{z} \left\{ C_F^F \left[ 2 \cdot \frac{1+z^2}{1-z+\Delta} \right] D_F^F\left(\frac{x}{z}\right) - 2 \cdot z^2 C_F^F \left( \frac{1+z^2}{1-z+\Delta} + \frac{(1-z)^2+1}{z} \right) D_F^F(x) \right\} = \\ &= \frac{\alpha_s}{2\pi} \int_0^1 \frac{dz}{z} \left\{ C_F^F \left[ \frac{1+z^2}{1-z+\Delta} \right] D_F^F\left(\frac{x}{z}\right) - z C_F^F \left( \frac{2}{1-z+\Delta} - \frac{3}{2} - 3z + \frac{3}{2} \right) D_F^F(x) \right\} = \\ &= \frac{\alpha_s}{2\pi} \int_0^1 \frac{dz}{z} \left\{ C_F^F \left[ \frac{1+z^2}{1-z+\Delta} \right] D_F^F\left(\frac{x}{z}\right) - z C_F^F \left( \frac{2}{1-z+\Delta} - \frac{3}{2} \right) D_F^F(x) \right\} - \underbrace{D_F^F(x) \frac{\alpha_s}{2\pi} \int_0^1 dz C_F^F \left( -3z + \frac{3}{2} \right)}_{=0} \end{aligned} \quad (\text{F6})$$

Since the integral converges we can set  $\Delta = 0$  and we see the two equations coincide.

#### b. The non-Singlet Case.

Consider now the octet case. For brevity we suppress the representation notation  $\alpha$  ([11] considers only the octet representation). The comparison of the two of the evolution equations in this case would be more tricky. This is because [11] uses the normalization scale  $\mu$  which is integrated

from the lower cut-off (in [11] it is  $\Lambda_{QCD}$  while in our case it's the splitting scale  $k$ ) to the hard scale  $Q$  while in this paper we write the evolution in term of the hard scale  $Q$ . The evolution equation in [11] is (e.g eq. 14 in that paper):

$$\frac{\partial \overline{D}_F^F(x, \mu)}{\partial \ln(\mu)} = \frac{\alpha_s}{\pi} \int_x^1 \frac{dz}{z} C_F^F P_{qq}(z) D_F^F\left(\frac{x}{z}, \mu\right) + \frac{\alpha_s}{\pi} N \left[ \ln\left(\frac{\mu}{Q}\right) + \frac{3}{4} \right] \overline{D}_F^F(x). \quad (\text{F7})$$

Actually the denominator in the logarithm of [11] is  $p_1^-$  (defined in that paper) rather than  $Q$  but they are of the same order of magnitude so in NLO we can use either. In order to go from  $\mu$  evolution to  $Q$  evolution we shall integrate this equation and then differentiate it with respect for  $Q$ , i.e:

$$\overline{D}_F^F(x, k^2, Q^2) = \int_{\ln(k)}^{\ln(Q)} \frac{\partial \overline{D}_F^F(x, \mu)}{\partial \ln(\mu)} d\ln(\mu), \quad (\text{F8})$$

and then

$$\frac{\partial \overline{D}_F^F(x, k^2, Q^2)}{\partial \ln(Q)} = \frac{\partial}{\partial \ln(Q)} \int_{\ln(k)}^{\ln(Q)} \frac{\partial \overline{D}_F^F(x, \mu)}{\partial \ln(\mu)} d\ln(\mu). \quad (\text{F9})$$

The first term of (F7) as well as the  $\frac{3}{4}$  part are  $Q$  independent and are therefore trivial to compute. The only non-trivial term is the one proportional to  $\ln\left(\frac{\mu}{Q}\right)$  for which we compute:

$$\frac{\partial}{\partial \ln(Q)} \int_{\ln(k)}^{\ln(Q)} \ln\left(\frac{\mu}{Q}\right) d\ln(\mu) = \frac{\partial}{\partial \ln(Q)} \left( -\frac{1}{2} \ln^2\left(\frac{k}{Q}\right) \right) = \ln\left(\frac{k}{Q}\right) \quad (\text{F10})$$

So we see that the evolution equation of [11] can be written in term of  $Q$  rather than  $\mu$  as:

$$\frac{\partial \overline{D}_F^F(x)}{\partial \ln(Q^2)} = \frac{\alpha_s}{2\pi} N \left[ \ln\left(\frac{k^2}{Q^2}\right) + \frac{3}{4} \right] \overline{D}_F^F(x) + \frac{\alpha_s}{2\pi} \int_x^1 \frac{dz}{z} \overline{C}_F^F P_{qq}(z) \overline{D}_F^F\left(\frac{x}{z}\right) \quad (\text{F11})$$

In DDT scheme however:

$$\frac{\partial \overline{D}_F^F(x)}{\partial \ln(Q^2)} = \frac{\alpha_s}{4\pi} \int_0^1 \frac{dz}{z} \overline{\Phi}_F^F(z) \overline{D}_F^F\left(\frac{x}{z}\right) - z^2 \overline{D}_F^F(x) (\Phi_F^F(z) + \Phi_F^G(z)) = \quad (\text{F12})$$

$$\begin{aligned}
&= \frac{\alpha_s}{2\pi} \int_0^1 \frac{dz}{z} \overline{C}_F^F \left[ \frac{1+z^2}{1-z+\Delta} \right] \overline{D}_F^F \left( \frac{x}{z} \right) - z^2 C_F^F \left( \frac{1+z^2}{1-z+\Delta} + \frac{(1-z)^2+1}{z} \right) \overline{D}_F^F(x) = \\
&= \frac{\alpha_s}{2\pi} \int_0^1 \frac{dz}{z} \overline{C}_F^F \left[ \frac{1+z^2}{1-z+\Delta} \right] \overline{D}_F^F \left( \frac{x}{z} \right) - z^2 \overline{C}_F^F \left( \frac{1+z^2}{1-z+\Delta} + \frac{(1-z)^2+1}{z} \right) \overline{D}_F^F(x) - \\
&\quad \overline{D}_F^F(x) \frac{\alpha_s}{2\pi} \int_0^1 dz z \left( C_F^F - \overline{C}_F^F \right) \left( \frac{1+z^2}{1-z+\Delta} + \frac{(1-z)^2+1}{z} \right)
\end{aligned}$$

The first integral is just the new kernel as in [11] (after we set  $\Delta = 0$ ), The second integral can be calculated analytically and we have (to leading order in  $\Delta$ ):

$$\begin{aligned}
\frac{\partial \overline{D}_F^F(x)}{\partial \ln(Q^2)} &= \frac{\alpha_s}{2\pi} \int_x^1 \frac{dz}{z} \overline{C}_F^F P_{qq}(z) \overline{D}_F^F \left( \frac{x}{z} \right) + \overline{D}_F^F(x) \frac{\alpha_s}{2\pi} \left( C_F^F - \overline{C}_F^F \right) \left( \frac{3}{2} + 2 \cdot \log \left( \frac{k^2}{Q^2} \right) \right) = \quad (\text{F13}) \\
&= \frac{\alpha_s}{2\pi} \int_x^1 \frac{dz}{z} \overline{C}_F^F P_{qq}(z) \overline{D}_F^F \left( \frac{x}{z} \right) + \overline{D}_F^F(x) \frac{\alpha_s}{2\pi} N \left( \frac{3}{4} + \log \left( \frac{k^2}{Q^2} \right) \right)
\end{aligned}$$

This is just Equation F11. We see that also in the non-singlet case both regularisation schemes lead to identical equations.

### c. Different Sudakov Factors

As we have seen in the previous subsection the evolution functions is the same, at least including the NLO logarithms, and therefore any observable arising from it must be the same. On the other hand we define the Sudakov factor as in (9). When expanding this expression to NLO for quark evolution (at  $N = 3$ ) we have:

$$\overline{S}_{8_A} = e^{-\sum_C (C_F^C - \overline{C}_F^C)} \int_{k_0^2}^{Q^2} \frac{dk^2}{k^2} \frac{\alpha_s(k^2)}{4\pi} \int_0^1 dz z V_F^C(z) = e^{-\int_{k_0^2}^{Q^2} \frac{dk^2}{k^2} \frac{\alpha_s}{4\pi} N \left( \frac{137}{54} + 2 \cdot \log \left( \frac{k^2}{Q^2} \right) \right)}. \quad (\text{F14})$$

This is similar in LO but different in NLO then the “extra” logarithms given in (F13) which should give:

$$\overline{S}_{8_A} = e^{-\left( C_F^F - \overline{C}_F^F \right) \int_{k_0^2}^{Q^2} \frac{dk^2}{k^2} \frac{\alpha_s(k^2)}{4\pi}} \int_0^1 dz z \sum_C V_F^C(z) = e^{-\int_{k_0^2}^{Q^2} \frac{dk^2}{k^2} \frac{\alpha_s}{4\pi} N \left( \frac{3}{2} + 2 \cdot \log \left( \frac{k^2}{Q^2} \right) \right)}.$$

This is due to the different way we chose to define the tree-level evolution equation (compare Eq. (10) and (F12) to the first part of Eq. (F13)), which “absorbs” some of the NLO logs. We stress again that once multiplying the solutions of (10) with the Sudakov factor (9) we’ll get the same distributions to NLO as if we solved (F13).

## 2. Regularization of $z \rightarrow 1$ divergence

Let us now discuss the regularisation in section IID. We use the fundamental solutions of evolution equations/the Green function, that are singular in  $x \rightarrow 1$  limit. On the other hand, the evolution equations themselves are not singular [8, 11], and it is easy to check that solving these evolution equations does not involve singularities. It’s natural to ask then whether these divergences, encountered in section IID, are physical or are purely the mathematical artifact of our method of computing  $[_1]\overline{D}$ , using Green functions. If so, does the regularization method introduced gives the same results as other methods?

In the following, we’ll show that these divergences are of mathematical nature and that our method of regularizing them gives the same result as a different approach to this problem, that avoids singularities altogether.

First let’s outline another method for the computation of  $[_1]\overline{D}$ . Let  $F_k(x_1, x_2, q_1, q_2)$  be the distribution that resulted from splitting at a scale  $k$ , i.e:

$${}^\alpha F_k^{AB}(x_1, x_2, q_1 = k, q_2 = k) = \sum_E \frac{\alpha_s(k^2)}{2\pi} G_h^E(x_1 + x_2, k^2) V_E^A(x_1 + x_2) \frac{n_A \alpha \overline{C}_A^B}{n_E} \quad (\text{F15})$$

Note that the parton type notation is consistent with that appearing in Eqs. (28-32). It’s now possible to perform the evolution in  $q_1$  and  $q_2$  up to to  $Q_1$  and  $Q_2$ . The evolution equation for  ${}^\alpha_{[1]}F_k^{AB}$  is actually just (10) but in each of the variables  $x_i, Q_i$  alone [11, 15, 17]:

$$\frac{\partial^\alpha F_k^{AB}(x_i, q_i)}{\partial q_i} = \frac{\alpha_s(q_i^2)}{4\pi} \sum_C \int_0^1 \frac{dz}{z} \left[ \alpha \overline{\Phi}_C^A(z) {}^\alpha F_k^{CB}\left(\frac{x_i}{z}, q_i\right) - z^{2\alpha} \overline{\Phi}_C^A(z) {}^\alpha F_k^{CB}(x_i, q_i) \right]. \quad (\text{F16})$$

There is also a rapidity evolution, but as explained before, it only contributes single logarithmic corrections to the Sudakov factor. We also need to add the effect of the Sudakov factors and to integrate over the initial splitting scale  $k$ , so we find that:



$${}_{[1]}^{\alpha}\bar{D}_h^{AB}(x_1, x_2, Q_1, Q_2) = \int_{Q_0^2}^{\min(Q_1^2, Q_2^2)} \frac{dk^2}{k^2} {}^{\alpha}\bar{S}_A(k^2, Q_1^2) {}^{\alpha}\bar{S}_B(k^2, Q_2^2) {}^{\alpha}F_k^{AB}(x_1, x_2, Q_1, Q_2). \quad (\text{F17})$$

Since (F16) has no divergences in it, even for  ${}^{\alpha}\bar{C}_A^B < 0$ ,  $F_k$  is well defined without need for any regularization.  $F_k$  can be numerically evaluated at  $Q_1, Q_2$  for every  $k$  using numerical methods to solving PDE's. The integral in (F17) can then be computed numerically using the values of  $F_k$  for each  $k$ .

Does this method gives the same result as the regularization introduced in the text? Because (F17) is hard to compute numerically, we will demonstrate this in a toy model that leaves only the essential ingredients. Let  $\tilde{F}(x, k)$  be a function that satisfies

$${}^{\alpha}\tilde{F}(x, k = 1.4 \text{ GeV}) = \tilde{F}_0(x) \quad (\text{F18})$$

for some known function  $F_0$  and obeys the differential equation:

$$\frac{\partial {}^{\alpha}\tilde{F}(x, k)}{\partial k} = \frac{\alpha_s(k^2)}{4\pi} \int_0^1 \frac{dz}{z} \left[ {}^{\alpha}\bar{\Phi}_G^G(z) {}^{\alpha}\tilde{F}\left(\frac{x}{z}, k\right) - z^{2\alpha} \bar{\Phi}_G^G(z) {}^{\alpha}\tilde{F}(x, k) \right], \quad (\text{F19})$$

i.e containing only gluon evolution. These assumptions simplify the numerical computations greatly while still keeping the problem of negative color factor for  $\alpha = 27$ . We'll now evaluate  $\tilde{F}$  for several values of  $k$  using the two methods. First using the fundamental solutions (we had to modify the solutions given in Appendix C to include only gluon evolution, i.e by setting  ${}^{\alpha}\bar{C}_F^F = {}^{\alpha}\bar{C}_G^G = {}^{\alpha}\bar{C}_F^G = 0$ ) we write:

$${}^{\alpha}\tilde{F}(x, k) = \int_0^1 \frac{dz}{z} {}^{\alpha}\tilde{F}_0(z) {}^{\alpha}\tilde{D}\left(\frac{x}{z}, k\right). \quad (\text{F20})$$

For  $\alpha = 27$  this integral diverges and we use the 1d version of the regularization given in section IID. On the other hand we directly evaluated (F19) using the Runge–Kutta method with  $k$  spacing of 0.025 [GeV] (a similar numerical methods as was used in [11, 17]). The results for  $F_0 = 6 \cdot x(1-x)$  at  $k = 1.5, 10, 30$  [GeV] for both  $\alpha = 27$  and the singlet channel (which is used as a consistency test) are shown in Fig. 25. It should be stressed that the fact that  $\tilde{F}$  can be negative for non-singlet channels is not a surprise [17].

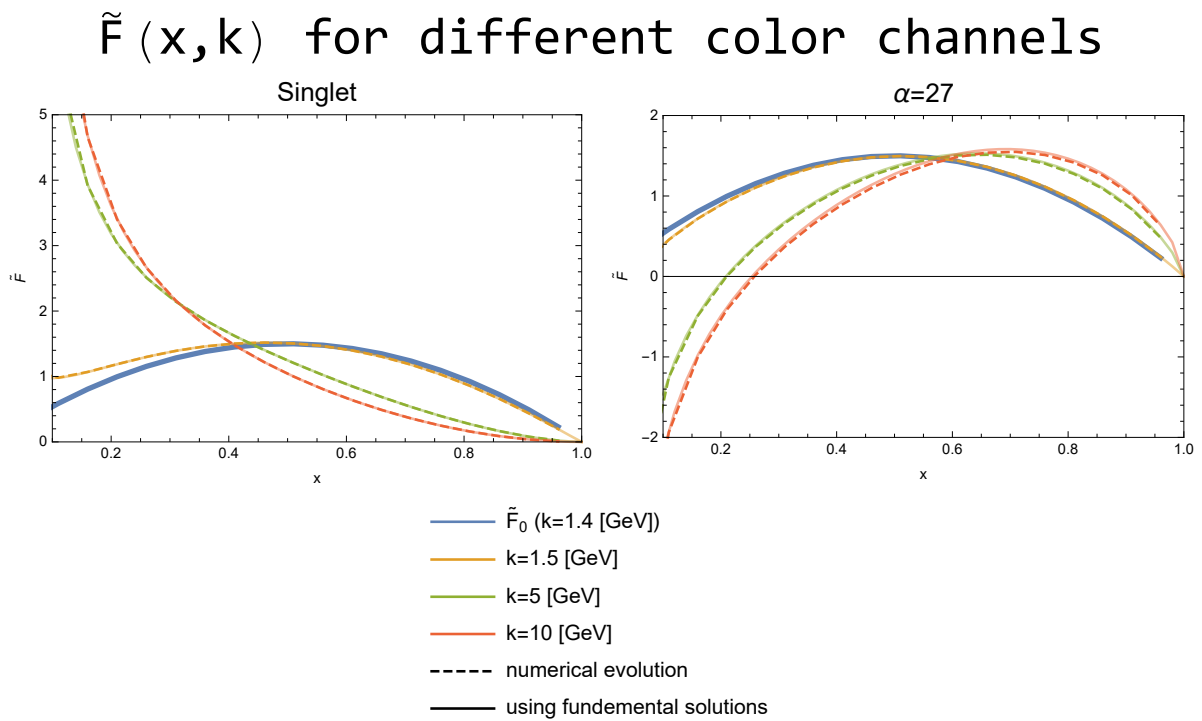


Figure 25. Comparison of the numerical evolution to the fundamental solution method. It can be seen that the results of both methods match.

We see that the two methods produce the same results. Because the use of fundamental solutions is much easier numerically (once they were computed) and also keeps the physical picture more transparent, we adopt this method in this paper.

- 
- [1] N. Paver and D. Treleani, *Nuovo Cim. A* **70**, 215 (1982).
  - [2] M. Mekhfi, *Phys. Rev. D* **32**, 2371 (1985).
  - [3] J. R. Gaunt and W. J. Stirling, *JHEP* **03**, 005 (2010), arXiv:0910.4347 [hep-ph].
  - [4] B. Blok, Y. Dokshitzer, L. Frankfurt, and M. Strikman, *Phys. Rev. D* **83**, 071501 (2011), arXiv:1009.2714 [hep-ph].
  - [5] M. Diehl, *PoS DIS2010*, 223 (2010), arXiv:1007.5477 [hep-ph].
  - [6] J. R. Gaunt and W. J. Stirling, *JHEP* **06**, 048 (2011), arXiv:1103.1888 [hep-ph].
  - [7] B. Blok, Y. Dokshitzer, L. Frankfurt, and M. Strikman, *Eur. Phys. J. C* **72**, 1963 (2012), arXiv:1106.5533 [hep-ph].
  - [8] M. Diehl, D. Ostermeier, and A. Schafer, *JHEP* **03**, 089 (2012), [Erratum: *JHEP* 03, 001 (2016)], arXiv:1111.0910 [hep-ph].
  - [9] B. Blok, Y. Dokshitzer, L. Frankfurt, and M. Strikman, *Eur. Phys. J. C* **74**, 2926 (2014), arXiv:1306.3763 [hep-ph].
  - [10] M. Diehl, J. R. Gaunt, and K. Schönwald, *JHEP* **06**, 083 (2017), arXiv:1702.06486 [hep-ph].
  - [11] A. V. Manohar and W. J. Waalewijn, *Phys. Rev. D* **85**, 114009 (2012), arXiv:1202.3794 [hep-ph].
  - [12] M. Mekhfi, *Phys. Rev. D* **32**, 2380 (1985).
  - [13] M. Mekhfi and X. Artru, *Phys. Rev. D* **37**, 2618 (1988).
  - [14] M. G. A. Buffing and P. J. Mulders, *Few Body Syst.* **56**, 337 (2015), arXiv:1410.6345 [hep-ph].
  - [15] M. G. A. Buffing, M. Diehl, and T. Kasemets, *JHEP* **01**, 044 (2018), arXiv:1708.03528 [hep-ph].
  - [16] M. Diehl, J. R. Gaunt, and P. Ploessl, *JHEP* **08**, 040 (2021), arXiv:2105.08425 [hep-ph].
  - [17] M. Diehl, J. R. Gaunt, P. Pichini, and P. Plöchl, *Eur. Phys. J. C* **81**, 1033 (2021), arXiv:2109.14304 [hep-ph].
  - [18] J. R. Gaunt, R. Maciula, and A. Szczurek, *Phys. Rev. D* **90**, 054017 (2014), arXiv:1407.5821 [hep-ph].
  - [19] M. Diehl, J. R. Gaunt, and K. Schönwald, *JHEP* **06**, 083 (2017), arXiv:1702.06486 [hep-ph].
  - [20] M. Diehl, F. Florian, and P. Ploessl, *JHEP* **02**, 229 (2024), arXiv:2310.16432 [hep-ph].
  - [21] Y. L. Dokshitzer, D. Diakonov, and S. I. Troian, *Phys. Rept.* **58**, 269 (1980).
  - [22] S. Frixione, P. Nason, and G. Ridolfi, *Nucl. Phys. B* **542**, 311 (1999), arXiv:hep-ph/9809367.
  - [23] I. Scimemi, *Adv. High Energy Phys.* **2019**, 3142510 (2019), arXiv:1901.08398 [hep-ph].
  - [24] J. Kodaira and L. Trentadue, *Phys. Lett. B* **112**, 66 (1982).
  - [25] Y. L. Dokshitzer, *Sov. Phys. JETP* **46**, 641 (1977).
  - [26] V. N. Gribov and L. N. Lipatov, *Sov. J. Nucl. Phys.* **15**, 438 (1972).

- [27] G. Altarelli and G. Parisi, Nucl. Phys. B **126**, 298 (1977).
- [28] A. Bassetto, M. Ciafaloni, and G. Marchesini, Phys. Rept. **100**, 201 (1983).
- [29] A. Vogt, Comput. Phys. Commun. **170**, 65 (2005), arXiv:hep-ph/0408244.
- [30] L. Frankfurt and M. Strikman, Phys. Rev. D **66**, 031502 (2002), arXiv:hep-ph/0205223.
- [31] M. Gluck, E. Reya, and A. Vogt, Z. Phys. C **67**, 433 (1995).
- [32] M. Glück, E. Reya, and A. Vogt, Eur. Phys. J. C **5**, 461 (1998), arXiv:hep-ph/9806404.
- [33] R. Kanwal, *Generalized Functions: Theory and Technique*, edited by Bellman (Academic Press, 1983).
- [34] I. Gel'fand and G. Shilov, *Generalized functions vol. 1*, edited by M. Agranovich (Academic Press, 1958).
- [35] T. Becher, A. Broggio, and A. Ferroglia, *Introduction to Soft-Collinear Effective Theory*, Vol. 896 (Springer, 2015) arXiv:1410.1892 [hep-ph].
- [36] R. K. Ellis, W. J. Stirling, and B. R. Webber, *QCD and collider physics*, Vol. 8 (Cambridge University Press, 2011).
- [37] V. Khachatryan *et al.* (CMS), JHEP **09**, 094 (2014), arXiv:1406.0484 [hep-ex].
- [38] J. C. Collins and D. E. Soper, Nucl. Phys. B **194**, 445 (1982).
- [39] J. R. Gaunt, JHEP **01**, 042 (2013), arXiv:1207.0480 [hep-ph].
- [40] Y. Dokshitzer, *QCD for begginers (draft)*.
- [41] Y. L. Dokshitzer and G. Marchesini, JHEP **01**, 007 (2006), arXiv:hep-ph/0509078.
- [42] P. Cvitanovic, *Group Theory: Birdtracks, Lie's, and Exceptional Groups* (PRINCETON UNIVERSITY PRESS, 2011).
- [43] B. L. Ioffe, V. S. Fadin, and L. N. Lipatov, *Quantum chromodynamics: Perturbative and nonperturbative aspects* (Cambridge Univ. Press, 2010).